

國立臺灣大學工學院化學工程學系



碩士論文

Department of Chemical Engineering

College of Engineering

National Taiwan University

Master Thesis

低溫多效蒸發海水淡化系統之最適化

Optimization of Multi-Effect Evaporation Desalination System  
for Low Grade Sensible Heat

江家諄

Jia-Juen Chiang

指導教授：陳誠亮 博士

Advisor: Cheng-Liang Chen, Ph.D.

中華民國 107 年 7 月

July, 2018

國立臺灣大學碩士學位論文  
口試委員會審定書



低溫多效蒸發海水淡化系統之最適化  
Optimization of Multi-Effect Evaporation  
Desalination System for Low Grade Sensible Heat

本論文係江家諄君 (R05524103) 在國立臺灣大學化學工程學系、所完成之碩士學位論文，於民國 107 年 7 月 13 日承下列考試委員審查通過及口試及格，特此證明

口試委員：

陳誠亮

(簽名)

(指導教授)

李端元

李國華

錢新怡

吳紀聖

系主任、所長

(簽名)

(是否須簽章依各院系所規定)



## 致謝

本論文得以完成首先要感謝我的恩師指導教授陳誠亮老師與提供許多建議的錢義隆老師及吳哲夫老師，在三位老師的教導及協助下，除了學習到書本的知識、解決問題的方法、做研究的態度還有處事的方式，本論文才得以順利完成，在此對三位老師致上最深的謝意。同時也感謝口試委員，台北科技大學李瑞元教授與台灣科技大學李豪業教授，在口試時提出鞭辟入裡的想法及建議，使本論文更加完整。

在程序系統工程實驗室的兩年中，特別感謝一起奮鬥的同窗，士寶、馬來西亞人(振濠)、易大師(均正)、孟凱、冠霖、彥翔及領導(哲安)，有你們陪伴與扶持，讓我在課業與研究方面都能順利度過。也感謝博士班小魚(柏毅)、Mike(馨右)、台柱(冠辰)，為實驗室樹立良好的學長姐風範，特別感謝博士班惠楚學姐在Latex與GAMS的幫助。感謝已畢業的曉玲、沅煒、柏安、睿、子傑、榮傑、于誠及昆庭等學長姐，在碩一時給予我許多珍貴的經驗，少走點冤枉路。感謝學弟妹立軒、向炫、80G(少秋)、小精靈(瑋呈)、孝錚、銀吉、皓人、品勛、瑋萱及川川(咸圳)，實驗室因為有你們而充滿了快活的空氣。感謝研究室中全體人員，於就學期間的提攜照顧與幫忙。你們的陪伴讓兩年的研究生生活變得絢麗多彩。

感謝RKN眾人，威全、圻陽、柏安、都華、于勳、彥廷、東達、以安、劭恆、鈺婷與子翔，你們的陪伴橫跨了我的學士及碩士生涯，一同度過小事、大事、好事和壞事，求學之路因你們而完整。

最後，還要感謝給我的雙親，我才能無後顧之憂，將心力放在研究生活上。僅將此文獻給我的父母、師長、學長姐弟妹及好友們。



## 摘要

近年來，台灣南部的缺水壓力因氣候變化和水庫淤積變得更加險峻。海水淡化技術在必要時能夠緩解這個即將到來的問題並能夠持續供應民生及工業用淡水，其中，多效蒸發技術已經廣泛應用於海水淡化，並具有低電力消耗的特點。在這篇論文中，吾人首先建構多效蒸發系統的數學模型，並討論如何增加使用低溫顯熱之效率。該模型主要根據質量和能量平衡，為一個高度非線性的規劃問題。同時也對新的架構—增強型多效蒸發系統，基於廢熱性能比進行研究。廢熱性能比定義為餾出物的焓與熱源的可利用能量之比。對於傳統多效蒸發系統，廢熱的離開溫度仍高導致廢熱無法被有效利用。在討論廢熱性能比中，增強型多效蒸發系統優於傳統多效蒸發系統，同時更能降低其熱交換面積。增強型多效蒸發系統能夠在指定的低廢熱出口溫度下充分利用顯熱廢熱。此外，廢熱的出口溫度是選擇不同系統的關鍵要素。當指定的廢熱出口溫度高於傳統多效蒸發系統的最低可行溫度時，使用傳統多效蒸發系統將在產水效率更有優勢。

關鍵字：海水淡化、最適化、多效蒸發、非線性規劃



## Abstract

In recent years, water stress becomes more severe in southern Taiwan due to climate change and reservoir siltation. Desalination technology can mitigate this upcoming issue and supply fresh water persistently. Multi-Effect Evaporation (MEE) system is one of thermal desalination technologies which has features of high efficiency in power consumption. A mathematical model of MEE system is developed to effectively utilize the sensible low grade waste heat. The model is based on mass and energy balances and it is highly non-linear. Besides conventional configuration, an advanced process, namely the Boosted MEE (BMEE) is also investigated on the basis of waste heat performance ratio. Waste heat performance ratio is defined as the ratio of the enthalpy of the distillate to the maximum exploitable energy of the heat source. For MEE system, the leaving temperature of waste heat is quite high and waste heat can not be efficiently exploited. To improve the operating efficiency, BMEE system is studied and the results show that the BMEE system is superior to the conventional MEE system in both waste heat performance ratio (up to 8%) and heat transfer area (up to 14%). The BMEE system has shown the capability to fully utilize the sensible waste heat at specified low waste heat outlet temperature. Moreover, the outlet temperature of waste heat is the key to choose either MEE system or BMEE system in terms of fresh-water production. While the specified waste heat outlet temperature is higher than the lowest possible temperature of the MEE system, it becomes more appropriate to use the MEE system rather than the BMEE system.

**Keyword:** Desalination; Optimization; Multi-Effect Evaporation; Non-linear programming (NLP)





# Contents

口試委員會審定書	i
致謝	ii
摘要	iii
<b>Abstract</b>	<b>iv</b>
<b>List of Figures</b>	<b>viii</b>
<b>List of Tables</b>	<b>ix</b>
<b>Nomenclature</b>	<b>x</b>
<b>1 Introduction</b>	<b>1</b>
1.1 Water Scarcity . . . . .	1
1.2 Desalination Technologies . . . . .	2
1.3 MEE Brief Process Description . . . . .	4
1.4 Key Parameters . . . . .	7
1.5 Motivation . . . . .	8
<b>2 Design of Multi-Effect Evaporation Systems</b>	<b>10</b>
2.1 Problem Statement . . . . .	10
2.2 Assumptions . . . . .	12
2.3 Model Formulation . . . . .	13
2.3.1 Thermodynamics properties . . . . .	13
2.3.2 Evaporator . . . . .	14
2.3.3 Flash Box . . . . .	15
2.3.4 Preheater . . . . .	15
2.3.5 Mixing Box . . . . .	16
2.3.6 Additional formulations for first effect . . . . .	17
2.3.7 Additional formulations for last effect . . . . .	18
2.3.8 Operational Constrains . . . . .	19
2.3.9 NLP Formulation . . . . .	20
2.4 Illustrative Examples . . . . .	21
2.4.1 Case 1: Influence of increasing waste heat outlet temperature . . . . .	21
2.4.2 Case 2: Influence of reducing waste heat outlet temperature . . . . .	22

2.5	Summary	22
<b>3</b>	<b>Design of Boosted Multi-Effect Evaporation Systems</b>	<b>26</b>
3.1	Problem Statement	26
3.2	Model Formulation	28
3.2.1	Evaporator	28
3.2.2	Booster	28
3.2.3	Mixing Box	28
3.2.4	NLP Formulation	29
3.3	Illustrative Examples	30
3.3.1	Case 1: Influence of inlet temperature of heat source on booster	30
3.3.2	Case 2: Influences of inlet temperature of heat source and number of effects	34
3.4	Summary	36
<b>4</b>	<b>MEE/BMEE Systems for Waste Heat Recovery in Refinery</b>	<b>37</b>
4.1	Problem Statement	38
4.2	Model Formulation	38
4.2.1	Additional Models	38
4.2.2	NLP Formulation	39
4.3	Case Study	41
<b>5</b>	<b>Conclusion</b>	<b>49</b>
	<b>Bibliography</b>	<b>50</b>







# List of Figures

1.1	Water distribution on Earth. . . . .	1
1.2	Desalination technology market in 2014. . . . .	3
1.3	Four-effect forward feed MEE systems . . . . .	6
1.4	A four-effect forward feed BMEE system . . . . .	9
2.1	A general effect of a MEE system. . . . .	11
2.2	First effect of a MEE system. . . . .	11
2.3	Last effect of a MEE system. . . . .	12
2.4	Optimal solution for minimum mass flow rate of waste heat. . . . .	24
2.5	Increase in waste heat outlet temperature. . . . .	24
2.6	Reduction in waste heat outlet temperature. . . . .	25
3.1	A general effect of a BMEE system. . . . .	27
3.2	Last effect of a BMEE system. . . . .	27
3.3	Optimal solution of BMEE system for Case 1 ( $T_{W_1} = 75^\circ\text{C}$ ). . . . .	32
3.4	Optimal solution of BMEE system for Case 1 ( $T_{W_1} = 80^\circ\text{C}$ ). . . . .	32
3.5	Optimal solution of BMEE system for Case 1 ( $T_{W_1} = 85^\circ\text{C}$ ). . . . .	33
3.6	Optimal solution of BMEE system for Case 1 ( $T_{W_1} = 90^\circ\text{C}$ ). . . . .	33
3.7	Waste heat performance ratio against heat source temperature. . . . .	35
3.8	Heat transfer area against heat source temperature. . . . .	35
4.1	Typical crude preheat train with six waste hot streams. . . . .	37
4.2	Indirect MEE system. . . . .	42
4.3	Indirect BMEE system. . . . .	43
4.4	Direct MEE system and indirect MEE system. . . . .	43
4.5	Direct MEE system and indirect BMEE system. . . . .	44
4.6	Direct BMEE system and indirect MEE system. . . . .	44
4.7	Direct BMEE system and indirect BMEE system. . . . .	45
4.8	Details of indirect MEE system in Figure 4.2. . . . .	46
4.9	Details of indirect BMEE system in Figure 4.3. . . . .	46
4.10	Details of indirect MEE system in Figure 4.4 and Figure 4.6. . . . .	47
4.11	Details of indirect BMEE system in Figure 4.5 and Figure 4.7. . . . .	47
4.12	Details of direct MEE system in Figure 4.4 and Figure 4.5. . . . .	48
4.13	Details of direct BMEE system in Figure 4.6 and Figure 4.7. . . . .	48



# List of Tables

1.1	Comparison of seawater desalination methods. . . . .	3
2.1	Parameter values used for Chapter 2. . . . .	20
2.2	Comparison between optimal and Subsection 2.4.1 values . . . . .	21
2.3	Comparison between optimal and Subsection 2.4.2 values. . . . .	22
3.1	Parameter values used for Chapter 3. . . . .	29
3.2	Optimal values for different inlet temperature. . . . .	30
3.3	Detailed heat transfer areas. . . . .	34
4.1	Parameter values used for Chapter 4. . . . .	40
4.2	Comparison for different configurations. . . . .	42



# Nomenclature

## Set and Indices

$\mathcal{J}$	$\{j j \text{ is a effect, } j = 1, \dots, J\}$
b	booster
c	condensate
e	evaporate
f	flash
g	flashbox
h	heating
i	in
o	out
p	preheater
s	saturation
w	waste heat

## Parameters

$\Delta T_{\min}$	minimum temperature difference for first effect and preheaters, °C
$\Delta T_{\min}^e$	minimum temperature difference over the evaporator, °C
$\Delta T_{\min}^w$	minimum temperature difference between heating medium and waste heat, °C
$\lambda_j^*$	latent heat of water vapor, kJ/kg where $^* = \{e, f, g, p, w\}$
$\lambda_j$	latent heat of water vapor entering evaporator, kJ/kg
$BPE_j$	boiling point elevation, °C
$C_{p,*}$	heat capacity of water, kJ/K·kg where $^* = \{B_j, D_j^i, D_j^o, F_j, W_j, W_j^s\}$



- $C_{p,*}^{\text{kero}}$  heat capacity of kerosine, kJ/K·kg  
where  $*=\{W_j, W_j^s\}$
- $D^{\text{tot}}$  total distillate, kg/s
- $H_*$  enthalpy, kJ/kg  
where  $*=\{D_j, D_j^c, D_j^i, D_j^o, D_j^p\}$
- $Q_{\text{ind}}$  energy recovered by indirect system, MW
- $T^{\text{sea}}$  seawater temperature, °C
- $T_{\text{dir}}^{\text{inlet}}$  waste heat inlet temperature of direct system, °C
- $T_{\text{dir}}^{\text{outlet}}$  waste heat outlet temperature of direct system, °C
- $T_{\text{ind}}^{\text{inlet}}$  heat medium inlet temperature of indirect system, °C
- $T_{\text{ind}}^{\text{outlet}}$  heat medium outlet temperature of indirect system, °C
- $U^*$  heat transfer coefficient, kW/m<sup>2</sup>·°C,  
where  $*=\{b, e, h, p, w\}$
- $W_{\text{dir}}$  waste heat flow rate of direct system, kg/s
- $X^{\text{sea}}$  seawater concentration, ppm

### Variables

- $\text{LMTD}_j^*$  logarithmic mean temperature difference, °C  
where  $*=\{h, p, w\}$
- $A_1^*$  heat transfer area of first evaporator, m<sup>2</sup>C  
where  $*=\{h, w\}$
- $A_j^*$  heat transfer area, m<sup>2</sup>C  
where  $*=\{b, e, p\}$
- $B_j$  brine, kg/s
- $D_{\text{dir}}$  distillate production by direct system, kg/s
- $D_{\text{ind}}$  distillate production by indirect system, kg/s
- $D_j$  distillate from previous effect to next effect, kg/s
- $D_j^c$  distillate exiting evaporator, kg/s
- $D_j^i$  distillate entering flashbox, kg/s
- $D_j^o$  distillate exiting flashbox, kg/s
- $D_j^p$  distillate exiting preheater, kg/s



- $F_c$  seawater as cooling water, kg/s
- $F_j$  seawater, kg/s
- $T_*$  temperature, °C  
where  $*=\{B_j, D_j, D_j^c, D_j^i, D_j^o, D_j^p, F_j, V_j, V_j^e, V_j^f, V_j^g, V_j^p, V_j^w, W_j, W_j^s\}$
- $V_j$  vapor entering evaporator, kg/s
- $V_j^e$  vapor generated by evaporation in evaporator, kg/s
- $V_j^f$  vapor generated by flash evaporation in evaporator, kg/s
- $V_j^g$  vapor generated in flashbox, kg/s
- $V_j^p$  vapor entering preheater, kg/s
- $V_j^w$  vapor generated by waste heat, kg/s
- $W_{ind}$  heating medium flow rate of indirect system, kg/s
- $W_j$  waste heat flow rate, kg/s
- $X_*$  salt concentration, ppm,  
where  $*=\{B_j, F_j\}$



# Chapter 1

## Introduction

### 1.1 Water Scarcity

Water and energy are critical to human well-being and sustainable development. Both resources are strongly related and highly interlinked. The generation of energy determines the amount of water demanded to produce that energy. Simultaneously, available freshwater resources ensure water is adequate for energy production. The global water demand is estimated to increase by some 55% by 2050, mainly for growing demands from manufacturing (400%), thermal electricity generation (140%) and domestic use (130%) [1]. However, the groundwater depletion and the glacier retreat are threatening water resources.

Around 97% of all the water on Earth is seawater, whereas the available fresh water is less than 0.3% [2] as shown in Figure 1.1. To make matters worse, the water distribution varies greatly from country to country. In Persian Gulf nations, such as Kuwait, Bahrain

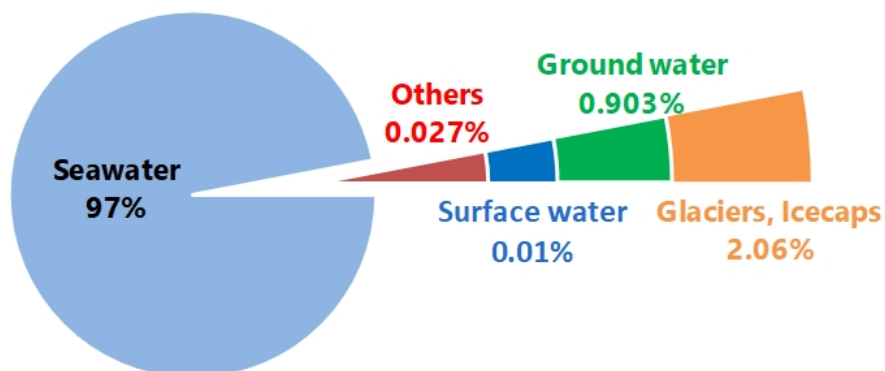


Figure 1.1: Water distribution on Earth.

and United Arab Emirates, had below 100 m<sup>3</sup> in renewable internal freshwater resources per capita while the values are about 3000 m<sup>3</sup> in east Asia [3]. It was reported that one-thirds of global population (2 billion people) live under conditions of severe water scarcity at least 1 month of the year [4,5]. Water Scarcity affects every continent and was warned in 2017 by the World Economic Forum: “notably extreme weather events and failure of climate change mitigation and adaptation as well as water crises – has emerged as a consistently central feature of the Global Risks Perception Survey (GRPS) risk landscape, strongly interconnected with many other risks, such as conflict and migration” [4]. To relief the tension of water stress, desalination is a promising approach in coastal countries.

## 1.2 Desalination Technologies

Desalination technologies can be classified into three major groups [6]:

1. **Thermal technologies** where evaporation and condensation are essential processes to generate fresh water. **The Multi Stage Flash (MSF)** is a process that vaporizes sea water by flashing part of the water at each effect. **Multi Effect Distillation (MED)**, also known as **Multi Effect Evaporation (MEE)**, is similar to MSF but unlike in which vapor from each effect is the driving force in the following stage.
2. **Membrane technologies** in which an applied pressure forces salty water through a membrane, leaving salts behind. In the **Reverse Osmosis (RO)**, an applied pressure is increased above the osmotic pressure, forcing the desalinated water to pass through the semi-permeable membranes. **Electrodialysis (ED)** is a process in which ions are transported through ion-exchange membranes under the influence of an applied electric potential.
3. **Hybrid processes** are results from the combination of 1. and 2.

Desalination technology market is given in Figure 1.2 [7]. A comparison of seawater desalination technologies is given in Table 1.1 [8]. Therein, RO holds the largest share

of desalination for several reasons: (i) moderate unit size compared with thermal desalination, (ii) modularity of installation, and (iii) low energy intensity. Despite various advantages of RO, about 70% of desalination in the Gulf Cooperation Council (GCC) is based on thermal processes. High operational tolerance is required in Arabian Gulf where the seawater have high salinity.

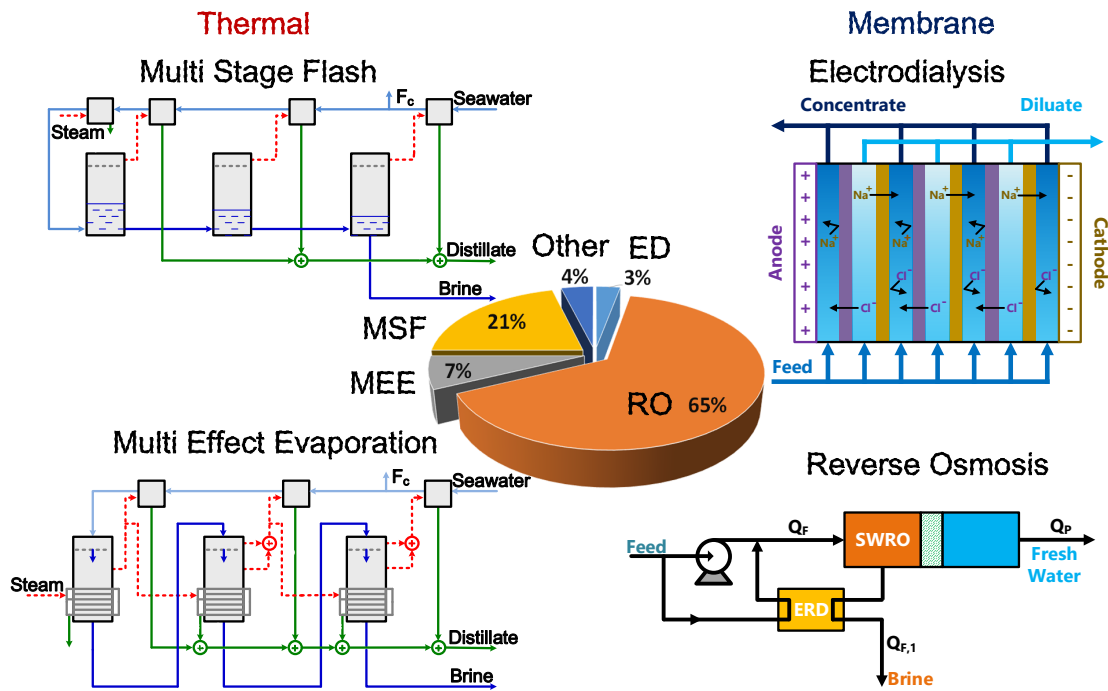


Figure 1.2: Desalination technology market in 2014.

Table 1.1: Comparison of seawater desalination methods.

	Unit	MSF	MEE	RO
Electrical energy	(kWh/m <sup>3</sup> )	4–6	1.2–2.5	3–5.5
Thermal energy	(kJ/kg)	190-390	230-390	None
Electrical equivalent for thermal energy	(kWh/m <sup>3</sup> )	9.5–19.5	5–8.5	None
Total equivalent electrical energy	(kWh/m <sup>3</sup> )	13.5–25.5	6.5–11	3–5.5
Distillate TDS	(mg/L)	<10	<10	<500
Operational tolerance		High	High	Low



### 1.3 MEE Brief Process Description

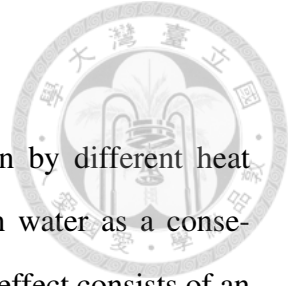


Figure 1.3 shows four-effect forward feed MEE systems driven by different heat sources. The primary component, evaporation effect, obtains fresh water as a consequence of the evaporation of seawater in the MEE system. A general effect consists of an evaporator, a flash box and a preheater.

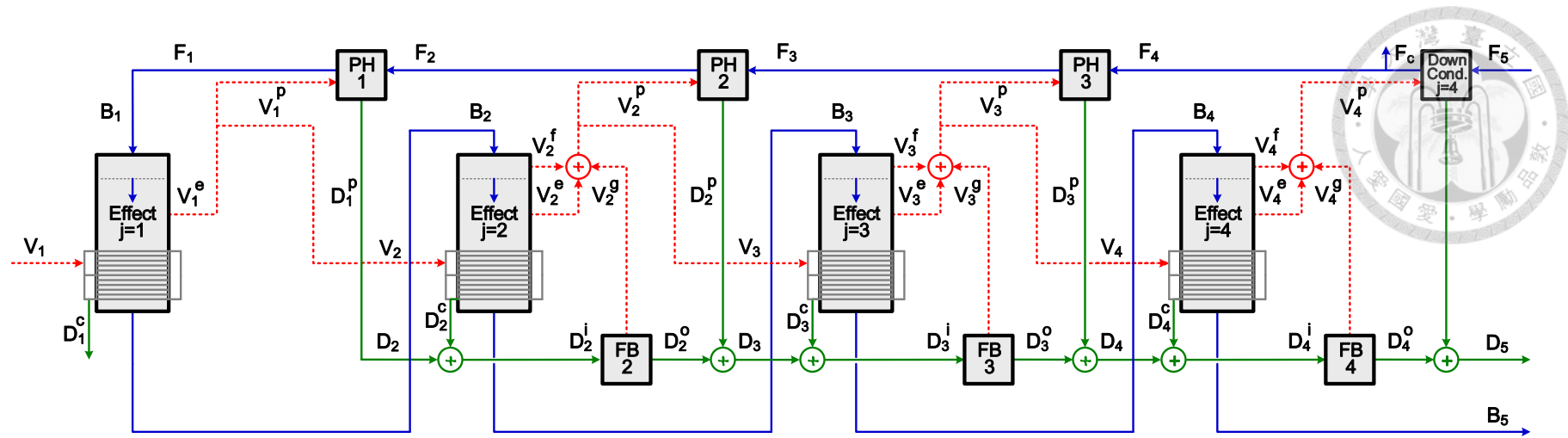
Based on the feed flow pattern, the MEE process can be operated in various configurations (forward feed, parallel feed and parallel/cross feed). In the forward feed system, both brine and heating medium flow in the same direction. The first effect is operated at the highest temperature and lowest salinity; thus, the forward feed system has the ability to operate at high top brine temperature [9]. The pressure and temperature of effect decrease gradually with increasing number of effect.

As Figure 1.3(a) shown, the seawater feed ( $F_1$ ) is sprayed into the the evaporator a series of evaporator tubes; heating medium ( $V_1$ ) releases the heat of vaporization to raise the temperature of seawater to saturation temperature ( $T_{B_2}$ ) and create vapor ( $V_1^e$ ). Next, part of  $V_1^e$  is sent to the first preheater to increase the seawater temperature from  $T_{F_1}$  to  $T_{F_2}$  and the unused vapor works as heating vapor in the second effect. The brine in the first effect ( $B_2$ ) goes to second effect as feed. Typically, the effect operates at a pressure which is marginally below the saturation pressure of the feed brine and causes the brine to flash evaporate ( $V^f$ ); therefore, vapor inside the evaporator effect is generated by two different ways, evaporation ( $V^e$ ) and flashing ( $V^f$ ). The distillate from both evaporator effect and preheater enters a flash box where the pressure is decreased to correspond with the pressure of the current effect, and result in another flashing vapor ( $V^g$ ). After that, part of the vapor of  $V^e$ ,  $V^f$  and  $V^g$  is used in preheater while the remaining vapor is supplied to the next effect as heating vapor.

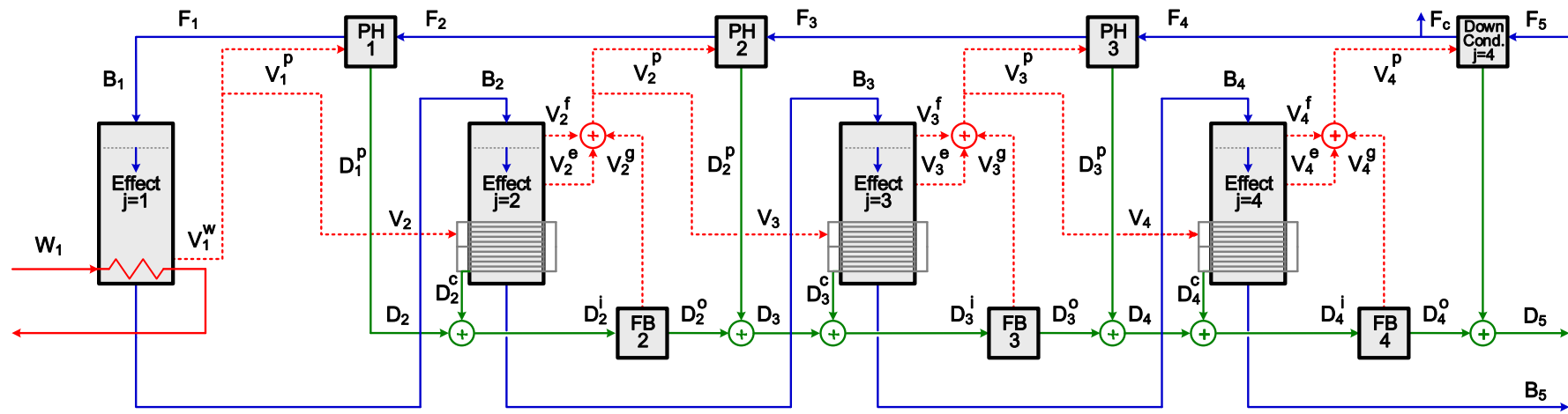
For the following effects, the processes of condensation, flashing, evaporation and heating described previously are repeated until the last effect. The vapors formed in the last effect ( $V^e$ ,  $V^f$  and  $V^g$ ) are condensed by the feed stream through the condenser and increase feed stream temperature from  $T^{\text{sea}}$  to  $T_{F_4}$ . Part of feed is rejected to the sea as

cooling water,  $F^c$ ; the remaining stream is consecutively heated by preheater [9–11].

Figure 1.3(b) represents a sensible heat driven forward feed MEE configuration. The operation of that is similar to the steam driven MEE system. The difference between these two process is the driving force of first evaporator. To distinguish between the two of them,  $V_1^c$  stands for the vapor generated by steam;  $V_1^w$  is representative of the vapor produced by sensible heat.



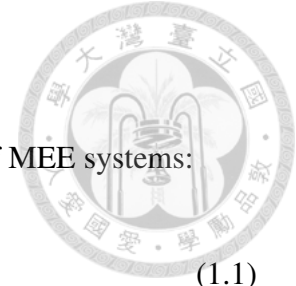
(a)



(b)

Figure 1.3: Four-effect forward feed MEE systems: (a) steam driven and (b) sensible heat driven

## 1.4 Key Parameters



The following parameters are used to analyze the performance of MEE systems:

$$\begin{aligned} \text{Performance Ratio (PR)} &\equiv \frac{\text{distillate heat}}{\text{actual waste heat}} && (1.1) \\ &= \frac{(\text{kg/s})_D \cdot \Delta h_{\text{ref.}}}{(\text{kg/s})_W \cdot \Delta h_{\text{act.}}} \\ &= \frac{(\text{kg/s})_D \cdot \Delta h_{\text{ref.}}}{(\text{kg/s})_W \cdot (h_{\text{wh,in}} - h_{\text{wh,out}})} \end{aligned}$$

$$\begin{aligned} \text{Waste Heat Performance Ratio (PR}_{\text{wh}}) &\equiv \frac{\text{distillate heat}}{\text{available waste heat}} && (1.2) \\ &= \frac{(\text{kg/s})_D \cdot \Delta h_{\text{ref.}}}{(\text{kg/s})_W \cdot \Delta h_{\text{ava.}}} \\ &= \frac{(\text{kg/s})_D \cdot \Delta h_{\text{ref.}}}{(\text{kg/s})_W \cdot (h_{\text{wh,in}} - h_{\text{con,in}})} \end{aligned}$$

where D is the distillate; W is the heating medium;  $\Delta h_{\text{ref.}}$  is the specific reference enthalpy of the distillate (as an industrial benchmark,  $\Delta h_{\text{ref.}} = 2333 \text{ kJ/kg}$ );  $\Delta h_{\text{act.}}$  is the total heat input into the system;  $\Delta h_{\text{ava.}}$  is the maximum exploitable energy of the heat source considering the lowest temperature which is the condenser inlet temperature [12–14].

Generally, performance ratio (PR) is to normalises distillate production based on the total heat input into the steam driven MEE systems. Nevertheless, it has been reported that performance ratio is not a suitable parameter to analyze the processes driven by a low grade sensible heat [13, 14]. With regard to maximum exploitation of waste heat energy, the waste heat performance ratio ( $\text{PR}_{\text{wh}}$ ) is more relevant to freshwater production in low grade sensible heat driven MEE system compared with the conventional performance ratio.

## 1.5 Motivation

Although the RO system consumes less energy, the MEE system is competitive when it utilizes waste heat from refinery or coal-fired power plant. The required energy of waste heat driven MEE system potentially reduce to 1.2–2.5 kWh/m<sup>3</sup>.

So far, many researchers have studied steam-driven MEE systems with diverse configurations. Few papers are found in the related literature [15–17] which have analyzed the MEE systems driven by low grade sensible heat. Low grade sensible heat that stems from renewable energies or process waste heat is commonly regarded as a promising heat source to power the relative energy intensive desalination processes. In 2011, a novel system scheme, the Boosted MED, also known as BMED or BMEE, has been proposed by Wang et al. [15] and successfully demonstrated by a pilot plant [18]. It has the ability to maximize exploitation of a sensible waste heat and increase the production of fresh water [12, 19].

Despite the elaborated researchs on the BMEE system done by Christ et al. [12, 13, 18, 20], Dastgerdi et al. [19] and Wang et al. [15], the scope of application is not discussed meticulously. This work aims to find out the optimal solution to utilize waste heat effectively with MEE system and BMEE system (as Figure ??(b) and Figure 1.4 respectively).





6

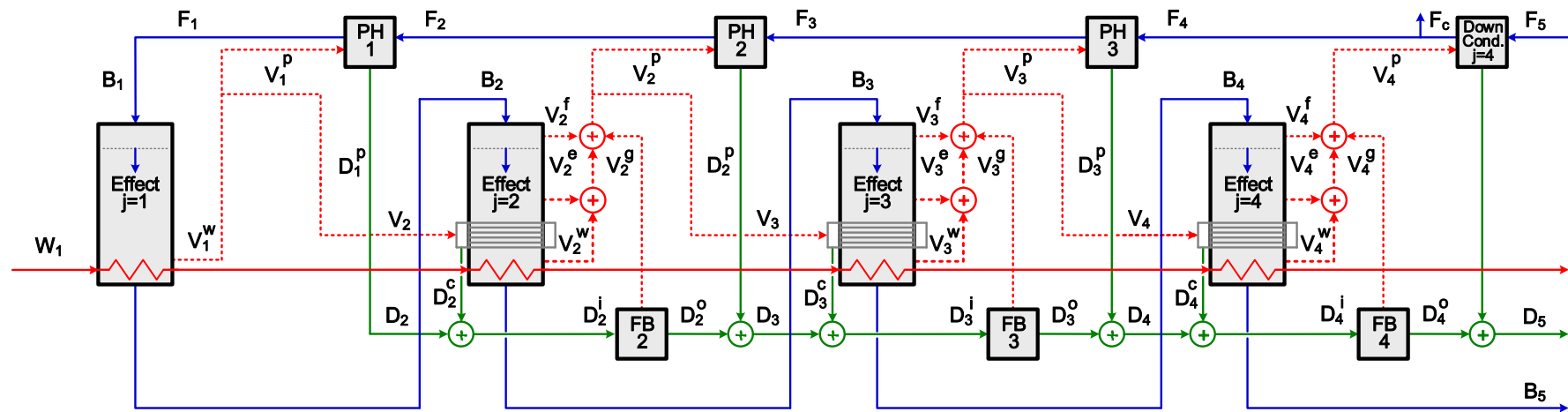


Figure 1.4: A four-effect forward feed BMEE system



## Chapter 2

# Design of Multi-Effect Evaporation Systems

### 2.1 Problem Statement

The steam driven MEE system is described in Section 1.3. However, we aim to fully utilize a low grade sensible heat. Therefore, an optimization of sensible heat driven MEE system is conducted. The schemes of a general effect, first effect and last effect are shown respectively in Figure 2.1, Figure 2.2 and Figure 2.3. Note that the heating medium is a bypass for general effect and last effect, it releases its sensible heat only in first evaporator. In this chapter, the heating medium is hot water and the feed is seawater.

Since a low grade sensible heat is chosen, the  $PR_{wh}$  in Section 1.4 will be discussed in the following chapters. For a given heating medium temperature and a fixed cooling water inlet temperature ( $T^{feed} = 26^{\circ}C$ ), the maximization of the  $PR_{wh}$  is only to minimize the mass flow rate of waste heat.

The influence of outlet temperature of heat source ( $T_{W_2}$ ) on the mass flow rate of waste heat is discussed in this chapter.

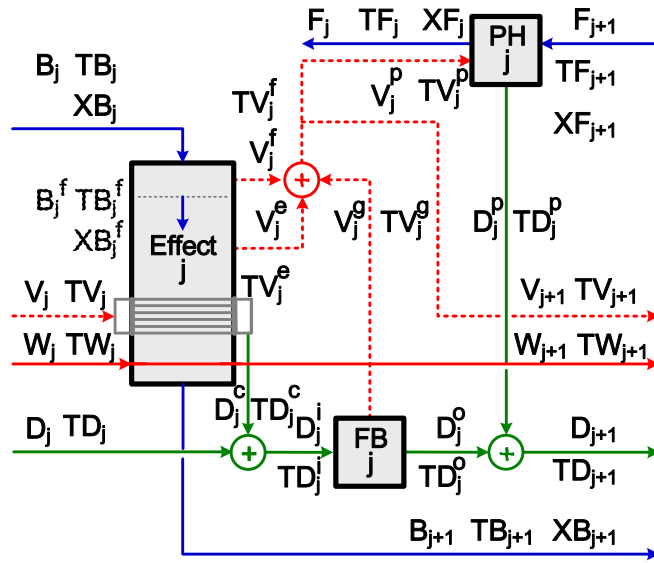


Figure 2.1: A general effect of a MEE system.

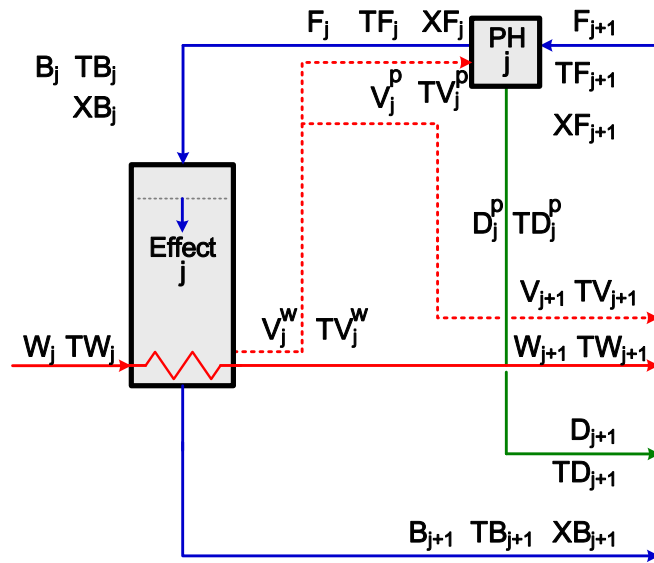


Figure 2.2: First effect of a MEE system.



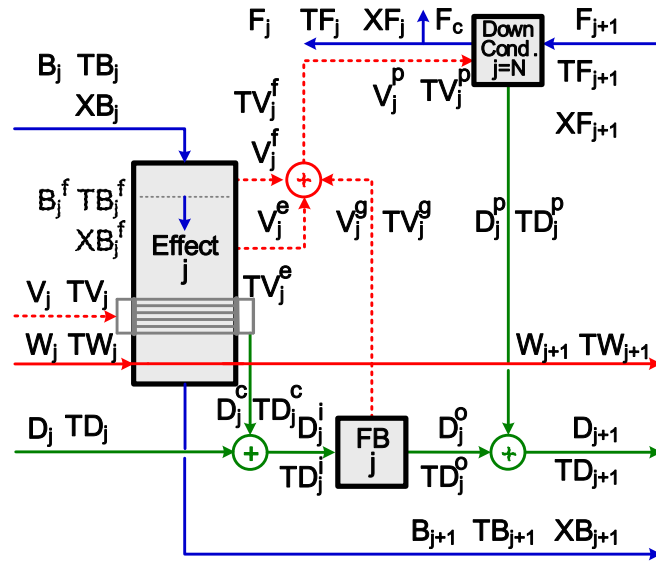


Figure 2.3: Last effect of a MEE system.

## 2.2 Assumptions

The following assumptions are used for model formulation of this thesis:

- The non-equilibrium allowance (NEA) is neglected, that is  $T_{B_j^f} = T_{B_{j+1}}$ .
- Pressure drop is neglected during the vapor condensation process .
- The effect of fouling factors and the presence of non-condensable gasses on the heat transfer coefficients in the evaporators, preheaters and the condenser are neglected. The heat transfer coefficients is assumed to be constant and identical over the process.
- The water vapor enter condenser, evaporators and preheaters are condensed to the saturation temperature.

## 2.3 Model Formulation

The model is based on the mass balance and energy balance according to Section 1.3, Figure 2.1, Figure 2.2 and Figure 3.2.



### 2.3.1 Thermodynamics properties

Enthalpy [kJ/kg] and Latent heat [kJ/kg] at  $T_j$  [°C]:

$$H = -0.033635409 + 4.207557011T_j - 6.200339 \times 10^{-4}T_j^2 + 4.459374 \times 10^{-6}T_j^3 \quad (2.1)$$

$$\lambda = 2501.897149 - 2.407064037T_j - 1.192217 \times 10^{-3}T_j^2 + 1.5863 \times 10^{-5}T_j^3 \quad (2.2)$$

BPE (Boiling point elevation) [°C] at  $T_j$  [°C] and  $X_{B_j}$  [ppm]:

$$\text{BPE} = X_{B_j}(b + cX_{B_j}) \quad (2.3)$$

with

$$b = (6.71 + 6.34 \times 10^{-2}T_j + 9.74 \times 10^{-5}T_j^2) \times 10^{-6}$$

$$c = (22.238 + 9.59 \times 10^{-3}T_j + 9.42 \times 10^{-5}T_j^2) \times 10^{-11}$$

The seawater specific heat capacity [kJ/K·kg] at  $T_j$  [°C] and  $X_{B_j}$  [ppm]:

$$C_p = (a + bT_j + cT_j^2 + dT_j^3) \quad (2.4)$$

with

$$\begin{aligned}
 a &= 4206.8 \times 10^{-3} - 6.6197 \times 10^{-6} X_{B_j} + 1.2288 \times 10^{-11} X_{B_j}^2 \\
 b &= -1.1262 \times 10^{-3} + 5.4178 \times 10^{-8} X_{B_j} - 2.2719 \times 10^{-13} X_{B_j}^2 \\
 c &= 1.2026 \times 10^{-5} - 5.3566 \times 10^{-10} X_{B_j} + 1.8906 \times 10^{-15} X_{B_j}^2 \\
 d &= 6.8777 \times 10^{-10} + 1.517 \times 10^{-12} X_{B_j} - 4.4268 \times 10^{-18} X_{B_j}^2
 \end{aligned}$$

### 2.3.2 Evaporator

Vapor is formed in general effect by two different mechanisms, evaporation ( $V^e$ ) and flashing ( $V^f$ ). The remaining brine ( $B_{j+1}$ ) flows into the next effect. The evaporator is operated at saturation temperature and the vapor (V) is condensed.

Mass balance for  $j \in \mathcal{J}$

$$B_j = V_j^f + V_j^e + B_{j+1} \quad (2.5)$$

$$B_j X_{B_j} = B_{j+1} X_{B_{j+1}} \quad (2.6)$$

$$V_j = D_j^c \quad (2.7)$$

$$W_j = W_{j+1} \quad (2.8)$$

Energy balance for  $j \in \mathcal{J}$

$$T_{V_j^f} = T_{B_{j+1}} \quad (2.9)$$

$$T_{V_j} = T_{D_j^c} \quad (2.10)$$

$$T_{V_j^e} = T_{B_{j+1}} - \text{BPE}_j \quad (2.11)$$

$$V_j^f \lambda_j^f = B_j (C_{p,B_j} T_{B_j} - C_{p,B_{j+1}} T_{B_{j+1}}) \quad (2.12)$$

$$V_j^e \lambda_j^e = V_j \lambda_j \quad (2.13)$$

Heat transfer area for  $j \in \mathcal{J}$

$$V_j^e \lambda_j^e = A_j^e U^e (T_{V_j} - T_{B_{j+1}}) \quad (2.14)$$



### 2.3.3 Flash Box

The distillate pressure is decreased in the flash boxes to correspond with the pressure of the current effect which causes a small fraction of the distillate to flash evaporate ( $V_j^g$ ).

Mass balance for  $j \in \mathcal{J}$

$$D_j^i = D_j^o + V_j^g \quad (2.15)$$

Energy balance for  $j \in \mathcal{J}$

$$T_{V_j^g} = T_{B_{j+1}} - \text{BPE}_j \quad (2.16)$$

$$T_{D_j^o} = T_{B_{j+1}} - \text{BPE}_j \quad (2.17)$$

$$V_j^g \lambda_j^g = D_j^i (C_{p,D_j^i} T_{D_j^i} - C_{p,D_j^o} T_{D_j^o}) \quad (2.18)$$

### 2.3.4 Preheater

Preheater is used to recover energy and reduce the energy required for heating the feed in the first effect. Part of vapor,  $V_j^e$ ,  $V_j^f$  and  $V_j^g$ , condensed and releases its heat to heat the feed.

Mass balance for  $j \in \mathcal{J}$

$$F_j = F_{j+1} \quad (2.19)$$

$$V_j^p = D_j^p \quad (2.20)$$

$$X_{F_j} = X_{F_{j+1}} \quad (2.21)$$

$$X_{F_j} = X^{\text{sea}} \quad (2.22)$$



Energy balance for  $j \in \mathcal{J}$

$$T_{D_j^p} = T_{B_{j+1}} - \text{BPE}_j \quad (2.23)$$

$$V_j^p \lambda_j^p = F_{j+1} (C_{p,F_j} T_{F_j} - C_{p,F_{j+1}} T_{F_{j+1}}) \quad (2.24)$$

Heat transfer area for  $j \in \mathcal{J}$

$$V_j^p \lambda_j^p = A_j^p U^p \text{LMTD}_j^p \quad (2.25)$$

$$\text{LMTD}_j^p = \frac{(T_{F_j} - T_{F_{j+1}})}{\ln \left( \frac{T_{V_j^p} - T_{F_{j+1}}}{T_{V_j^p} - T_{F_j}} \right)} \quad (2.26)$$

### 2.3.5 Mixing Box

The mixing box is only to recombine condensed distillate from previous effect, pre-heater and evaporator; or recombine vapor of  $V_j^c$ ,  $V_j^f$  and  $V_j^g$ .

Mass balance for  $j \in \mathcal{J}$

$$V_j^p + V_{j+1} = V_j^f + V_j^c + V_j^g \quad (2.27)$$

$$D_j^i = D_j + D_j^c \quad (2.28)$$

$$D_{j+1} = D_j^o + D_j^p \quad (2.29)$$

Energy balance for  $j \in \mathcal{J}$

$$V_j^p \lambda_j^p + V_{j+1} \lambda_{j+1} = V_j^f \lambda_j^f + V_j^c \lambda_j^c + V_j^g \lambda_j^g \quad (2.30)$$

$$D_j^i H_{D_j^i} = D_j H_{D_j} + D_j^c H_{D_j^c} \quad (2.31)$$

$$D_{j+1} H_{D_{j+1}} = D_j^o H_{D_j^o} + D_j^p H_{D_j^p} \quad (2.32)$$

### 2.3.6 Additional formulations for first effect



Since there are no vapor from previous effect, flash vapor ( $V^f$ ) and flash box. The following variables have to be zero.

For  $j = 1$

$$V_j = 0 \quad (2.33)$$

$$V_j^f = 0 \quad (2.34)$$

$$V_j^g = 0 \quad (2.35)$$

$$D_j = 0 \quad (2.36)$$

$$D_j^c = 0 \quad (2.37)$$

$$D_j^i = 0 \quad (2.38)$$

$$D_j^o = 0 \quad (2.39)$$

The mass balance and energy balance between preheater and first evaporator.

For  $j = 1$

$$B_j = F_j \quad (2.40)$$

$$X_{B_j} = X_{F_j} \quad (2.41)$$

$$T_{B_j} = T_{F_j} \quad (2.42)$$

Evaporator is driven by sensible heat, the heat is released for both heating and evaporation.

For  $j = 1$

$$T_{V_j^w} = T_{B_{j+1}} - \text{BPE}_j \quad (2.43)$$

$$W_j(C_{p,W_j}T_{W_j} - C_{p,W_j^s}T_{W_j^s}) = V_j^w\lambda_j^w \quad (2.44)$$

$$W_j(C_{p,W_j^s}T_{W_j^s} - C_{p,W_{j+1}}T_{W_{j+1}}) = B_j(C_{p,B_{j+1}}T_{B_{j+1}} - C_{p,B_j}T_{B_j}) \quad (2.45)$$

$$V_j^w\lambda_j^w = A_j^c U^c \text{LMTD}_j \quad (2.46)$$

$$B_j(C_{p,B_{j+1}}T_{B_{j+1}} - C_{p,B_j}T_{B_j}) = A_j^h U^h \text{LMTD}_j \quad (2.47)$$

$$\text{LMTD}_j^w = \frac{(T_{W_j} - T_{W_j^s})}{\ln \frac{(T_{W_j} - T_{B_{j+1}})}{(T_{W_j^*} - T_{B_{j+1}})}} \quad (2.48)$$

$$\text{LMTD}_j^h = \frac{(T_{W_j^*} - T_{B_{j+1}}) - (T_{W_{j+1}} - T_{B_j})}{\ln \frac{(T_{W_j^*} - T_{B_{j+1}})}{(T_{W_{j+1}} - T_{B_j})}} \quad (2.49)$$

### 2.3.7 Additional formulations for last effect

Total vapor is condensed by condenser. Part of feed leaves as cooling water.

For  $j = \mathcal{J}$

$$D_{j+1} = D^{\text{tot}} \quad (2.50)$$

$$F_{j+1} = F_j + F_c \quad (2.51)$$

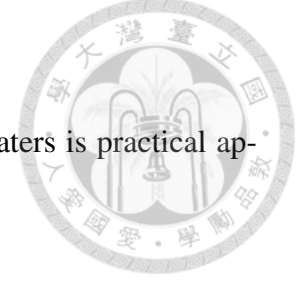
$$F_{j+1} = F^{\text{tot}} \quad (2.52)$$

$$V_{j+1} = 0 \quad (2.53)$$



### 2.3.8 Operational Constrains

Uniform heat transfer area distribution in evaporators and preheaters is practical application for ease of maintenance.



$$A_j^e = A_{j+1}^e \quad \text{for } j \in \mathcal{J}, j > 1 \quad (2.54)$$

$$A_j^p = A_{j+1}^p \quad \text{for } j \in \mathcal{J}, j < J - 1 \quad (2.55)$$

Boundary conditions and limits:

$$D^{\text{tot}} = D_{j+1} \quad \text{for } j = J \quad (2.56)$$

$$F_c \leq F_c^{\text{up}} \quad \text{for } j = J \quad (2.57)$$

$$X_{B_{j+1}} = X^{\text{up}} \quad \text{for } j = J \quad (2.58)$$

To avoid temperature crosses among stages, following constrain must be satisfied:

$$T_j > T_{j+1} \quad \text{for } j \in \mathcal{J}, j \neq J \quad (2.59)$$

Minimum evaporator temperature difference:

$$T_{B_j} - T_{B_{j+1}} \geq \Delta T_{\min}^e \quad \text{for } j \in \mathcal{J}, j > 1 \quad (2.60)$$

Minimum heat exchanger temperature difference:

$$T_{W_j^s} - T_{B_{j+1}} \geq \Delta T_{\min} \quad \text{for } j = 1 \quad (2.61)$$

$$T_{W_{j+1}} - T_{B_j} \geq \Delta T_{\min} \quad \text{for } j \in \mathcal{J} \quad (2.62)$$

$$T_{V_j^p} - T_{F_j} \geq \Delta T_{\min} \quad \text{for } j \in \mathcal{J} \quad (2.63)$$



### 2.3.9 NLP Formulation

Given a fixed number of effects, the proposed objective function for minimization is the mass flow rate of waste heat satisfying a specific fresh water demand.

Table 2.1 lists the parameter values used for Chapter 2.

$$\min_{x \in \Omega} \Phi = W_1$$

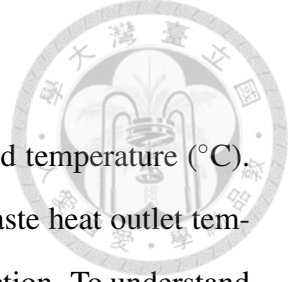
$$x \equiv \left\{ \begin{array}{l} A_j^e, A_1^h, A_j^p; \text{LMTD}_j^h, \text{LMTD}_j^p, \text{LMTD}_j^w; \\ V_j^e, V_j^f, V_j^g, V_j^p, V_j^w; \lambda_j, \lambda_j^e, \lambda_j^f, \lambda_j^g, \lambda_j^p, \lambda_j^w; \\ T_{V_j^e}, T_{V_j^f}, T_{V_j^g}, T_{V_j^p}, T_{V_j^w}; B_j, F_c, F_j, V_j, W_j; \\ T_{B_j}, T_{F_j}, T_{V_j}, T_{W_j}, T_{W_j^s}; X_{B_j}, X_{F_j}; \text{BPE}_j; C_p; \\ D_j, D_j^c, D_j^i, D_j^o, D_j^p; T_{D_j}, T_{D_j^c}, T_{D_j^i}, T_{D_j^o}, T_{D_j^p}; \\ U; H_{D_j}, H_{D_j^c}, H_{D_j^i}, H_{D_j^o}, H_{D_j^p}; \\ \forall j \in \mathcal{J} \equiv \{1, 2, \dots, J\} \end{array} \right\}$$

$$\Omega = \{x \mid \text{Eqs. (2.1)-(2.63)}\}$$

Table 2.1: Parameter values

Parameter	Unit	Value	Parameter	Unit	Value
$\Delta T_{\min}$	(°C)	2.00	$T_{W_1}$	(°C)	85.00
$\Delta T_{\min}^e$	(°C)	3.00	$T^{\text{sea } a}$	(°C)	26.00
$D^{\text{tot } a}$	(kg/s)	393.94	$X^{\text{sea } a}$	(ppm)	45,978.90
$F_c^{\text{up } a}$	(kg/s)	7283.55	$X^{\text{up } a}$	(ppm)	72,000.00
J	(-)	6	U <sup>a</sup>	(kW)/(m <sup>2</sup> °C)	3.00

<sup>a</sup>Numerical values from Druetta et al. [11]



## 2.4 Illustrative Examples

Figure 2.4 shows a optimal scheme with mass flow rate (kg/s) and temperature ( $^{\circ}\text{C}$ ). The minimum mass flow rate of waste heat is 1169.0 kg/s and the waste heat outlet temperature is  $57.2^{\circ}\text{C}$ . This optimal result is a benchmark case for this section. To understand how waste heat outlet temperature influences on waste heat flow rate, the following cases were optimized with Figure 2.4 scheme but different waste heat outlet temperature.

The simulations in this thesis were carried out by an advanced tool, General Algebraic Modeling System (GAMS). GAMS is a high-level modeling system for mathematical programming and optimization. It contains various NLP local solvers including CONOPT3, CONOPT4 and MINOS algorithms. The solver CONOPT is suggested by Druetta et al. [11]. This solver was used in this work and was successfully executed in a short CPU time. The model has 737 variables and 554 constraints. Global optimal solution cannot be guaranteed due to non-convex problem.

An Intel Core i7 6700 M 3.40 GHz processor with 16 GB RAM has been used to perform the simulations and optimizations.

### 2.4.1 Case 1: Influence of increasing waste heat outlet temperature

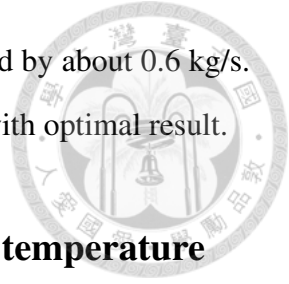
Figure 2.5 shows a result of increasing waste heat outlet temperature from  $57.2^{\circ}\text{C}$  to  $60^{\circ}\text{C}$ . Table 2.2 shows notable parameters considering both optimal and Case 1 results.

The waste heat leave the system with higher outlet temperature, that is, less heat is

Table 2.2: Comparison between optimal and Case 1 values

Parameter	Unit	Optimal	Case 1
$V_1^e$	(kg/s)	52.8	52.2
$W$	(kg/s)	1169.0	1281.7
$T_{W_2}$	( $^{\circ}\text{C}$ )	57.2	60.0
$\text{PR}_{\text{wh}}$	(-)	3.188	2.908

exploited by the system. In first effect, the vapor generation decreased by about 0.6 kg/s. Therefore, an increase in waste heat flow rate is required compared with optimal result.



### 2.4.2 Case 2: Influence of reducing waste heat outlet temperature

Figure 2.6 shows a result of reducing waste heat outlet temperature from 57.2°C to 56.9°C. This is the lowest possible waste heat outlet temperature that can be achieved in this system. Table 2.3 shows notable parameters considering both optimal and Case 2 results.

Though more waste heat is used in first evaporator compared with optimized case, the vapor generation is decreased by about 0.1 kg/s. The decrease in outlet temperature forces the temperature of the feed entering first evaporator ( $T_{F_1}$ ) to drop. Consequently, more energy is used for heating in first evaporator and that leads to the reduction in vapor. Therefore, an increase in waste heat flow rate is required compared with optimal result.

Table 2.3: Comparison between optimal and Case 2 values.

Parameter	Unit	Optimal	Case 2
$V_1^w$	(kg/s)	52.8	52.7
$W$	(kg/s)	1169.0	1171.0
$T_{W_2}$	(°C)	57.2	56.9
$PR_{wh}$	(-)	3.188	3.182

## 2.5 Summary

A deterministic NLP mathematical model has been developed to simulate and optimize the MEE system, which has ability to determine the optimal profiles of flow rate, heat transfer area, salinity and temperature. The influence of waste heat outlet temperature on waste heat performance ratio was investigated. It was observed that the optimal

waste heat outlet temperature were approaching the low bound of waste heat outlet temperature. However, the leaving temperature was quite high and the waste heat could not be efficiently exploited.



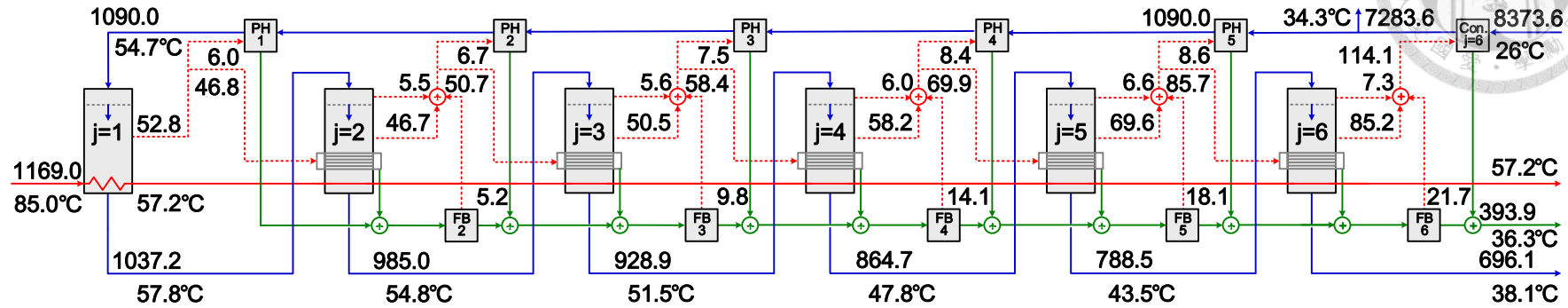
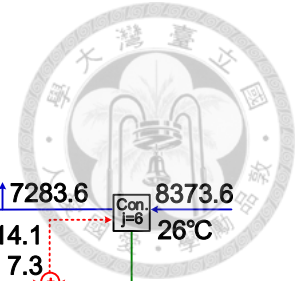


Figure 2.4: Optimal solution for minimum mass flow rate of waste heat.

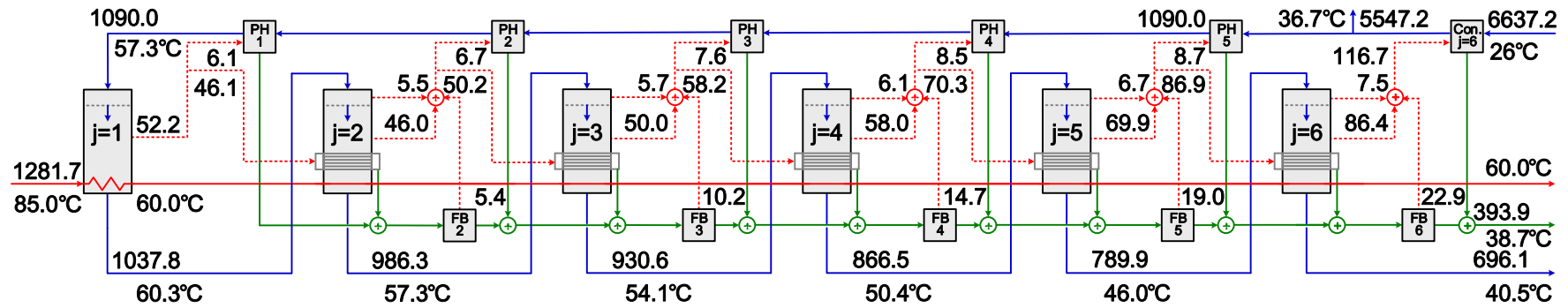


Figure 2.5: Increase in waste heat outlet temperature.

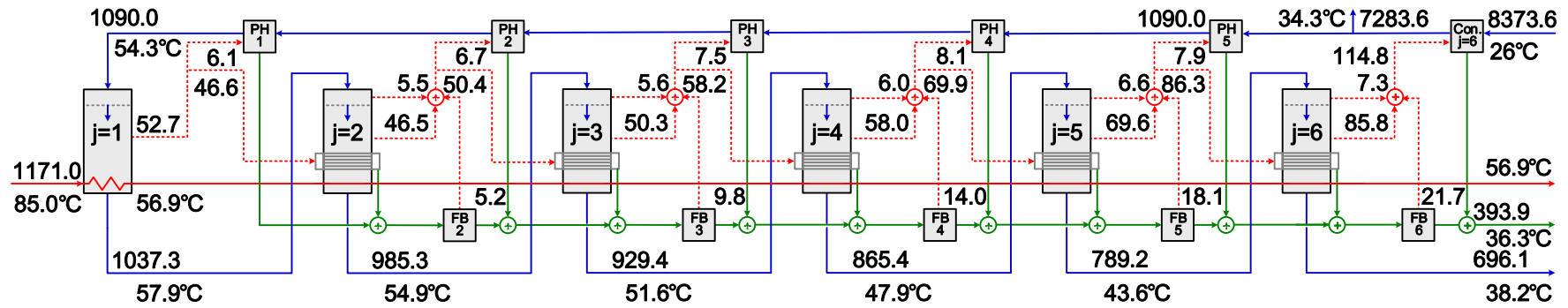


Figure 2.6: Reduction in waste heat outlet temperature.



## Chapter 3

# Design of Boosted Multi-Effect Evaporation Systems

The booster is designed to fully utilize a sensible waste heat. The scheme is slightly distinguished from Wang et al. [15], where the booster is an additional device outside the MEE system. In this work, the booster is a heat exchanger inside the evaporator and generates more vapor ( $V^w$ ). The difference between BMEE and MEE is that the heating medium releases its sensible heat in general effect and last effect by boosters, so first effect of BMEE system is identical to that of MEE system. The goal and solver of this chapter are the same as Chapter 3.

### 3.1 Problem Statement

The sensible heat driven MEE system is described in Chapter 2. To fully utilize a low grade sensible heat, an optimization of sensible heat driven BMEE system is conducted. The schemes of a general effect, first effect and last effect each are shown in Figure 3.1, Figure 2.2 and Figure 3.2, respectively. In this chapter, the heating medium is hot water and the cooling water is seawater.

Since a low grade sensible heat is chosen, the  $PR_{wh}$  in Section 1.4 will be discussed in the following chapters. For a given heating medium temperature and a fixed cooling water inlet temperature ( $T^{\text{feed}} = 26^\circ\text{C}$ ), the maximization of the  $PR_{wh}$  is only to minimize the mass flow rate of waste heat.

The influences of inlet temperature of heat source ( $T_{W_1}$ ) and number of effects on the mass flow rate of waste heat are discussed in this chapter.

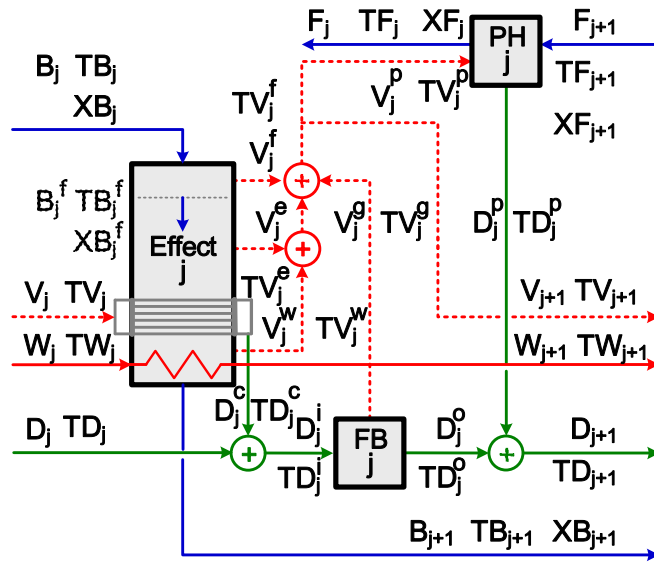


Figure 3.1: A general effect of a BMEE system.

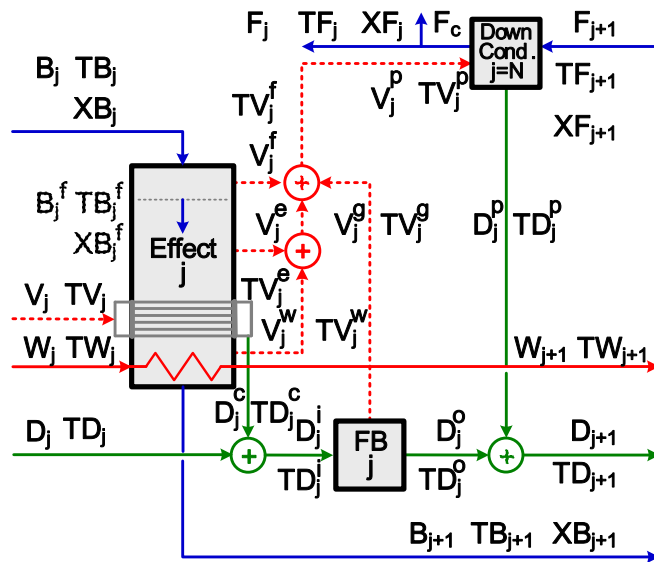


Figure 3.2: Last effect of a BMEE system.



## 3.2 Model Formulation

The model is based on the mass balance and energy balance according to Section 1.3, Figure 2.2, Figure 3.1 and Figure 3.2.



### 3.2.1 Evaporator

Eqs. (3.1) is proposed to replace the original Eqs. (2.5) for  $j \in \mathcal{J}, j > 1$

$$B_j = V_j^f + V_j^e + V_j^w + B_{j+1} \quad (3.1)$$

### 3.2.2 Booster

Energy balance for  $j \in \mathcal{J}, j > 1$

$$T_{V_j^w} = T_{B_{j+1}} - \text{BPE}_j \quad (3.2)$$

$$V_j^w \lambda_j^w = W_j (C_{p,W_j} T_{W_j} - C_{p,W_{j+1}} T_{W_{j+1}}) \quad (3.3)$$

Heat transfer area for  $j \in \mathcal{J}, j > 1$

$$V_j^w \lambda_j^w = A_j^b U^b \text{LMTD}_j^w \quad (3.4)$$

$$\text{LMTD}_j^w = \frac{(T_{W_j} - T_{W_{j+1}})}{\ln \frac{(T_{W_j} - T_{B_{j+1}})}{(T_{W_{j+1}} - T_{B_{j+1}})}} \quad (3.5)$$

### 3.2.3 Mixing Box

Eqs. (3.6) and Eqs. (3.7) are proposed to replace the original Eqs. (2.27) and Eqs. (2.30) for  $j \in \mathcal{J}, j > 1$

$$V_j^p + V_{j+1} = V_j^f + V_j^e + V_j^g + V_j^w \quad (3.6)$$

$$V_j^p \lambda_j^p + V_{j+1} \lambda_{j+1} = V_j^f \lambda_j^f + V_j^e \lambda_j^e + V_j^g \lambda_j^g + V_j^w \lambda_j^w \quad (3.7)$$



### 3.2.4 NLP Formulation

Given a fixed number of effects, the proposed objective function for minimization is the mass flow rate of waste heat satisfying a specific fresh water demand.

Table 3.1 lists the parameter values used for Chapter 3.

$$\min_{x \in \Omega} \Phi = W_1$$

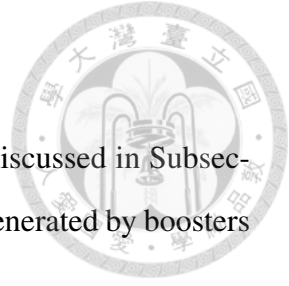
$$x \equiv \left\{ \begin{array}{l} A_j^b, A_j^e, A_1^h, A_j^p; \text{LMTD}_j^h, \text{LMTD}_j^p, \text{LMTD}_j^w; \\ V_j^e, V_j^f, V_j^g, V_j^p, V_j^w; \lambda_j, \lambda_j^e, \lambda_j^f, \lambda_j^g, \lambda_j^p, \lambda_j^w; \\ T_{V_j^e}, T_{V_j^f}, T_{V_j^g}, T_{V_j^p}, T_{V_j^w}; B_j, F_c, F_j, V_j, W_j; \\ T_{B_j}, T_{F_j}, T_{V_j}, T_{W_j}, T_{W_j^s}; X_{B_j}, X_{F_j}; \text{BPE}_j; C_p; \\ D_j, D_j^c, D_j^i, D_j^o, D_j^p; T_{D_j}, T_{D_j^c}, T_{D_j^i}, T_{D_j^o}, T_{D_j^p}; \\ U; H_{D_j}, H_{D_j^c}, H_{D_j^i}, H_{D_j^o}, H_{D_j^p}; \\ \forall j \in \mathcal{J} \equiv \{1, 2, \dots, J\} \end{array} \right\}$$

$$\Omega = \{x \mid \text{Eqs. (2.1)-(2.26), Eqs. (2.28)-(2.29), Eqs. (2.31)-(2.63), Eqs. (3.1)-(3.7)}\}$$

Table 3.1: Parameter values.

Parameter	Unit	Value	Parameter	Unit	Value
$\Delta T_{\min}$	(°C)	2.00	$T_{W_1}$	(°C)	65.00-95.00
$\Delta T_{\min}^e$	(°C)	3.00	$T^{\text{sea } a}$	(°C)	26.00
$D^{\text{tot } a}$	(kg/s)	393.94	$X^{\text{sea } a}$	(ppm)	45,978.90
$F_c^{\text{up } a}$	(kg/s)	7283.55	$X^{\text{up } a}$	(ppm)	72,000.00
J	(-)	5-7	U <sup>a</sup>	(kW)/(m <sup>2</sup> °C)	3.00

<sup>a</sup> Numerical values from Druetta et al. [11]



### 3.3 Illustrative Examples

The influence of inlet temperature of heat source on boosters is discussed in Subsection 3.3.1. The varied positions of boosters and the amount of vapor generated by boosters ( $V_j^w$ ) are essential to understanding.

The influences of inlet temperature of heat source and number of effects on waste heat performance ratio is investigated in Subsection 3.3.2. The inlet temperature of heat source varies from 65°C to 95°C and number of effects changes from 5 to 7. The BMEE system is benchmarked against the MEE system formulated in Chapter 2.

#### 3.3.1 Case 1: Influence of inlet temperature of heat source on booster

Figure 3.3, Figure 3.4, Figure 3.5 and Figure 3.6 illustrate the optimal designs where inlet temperature of heat source are respectively 75°C, 80°C, 85°C and 90°C. Table 3.2 shows optimal values for different inlet temperature.

Table 3.2: Optimal values for different inlet temperature.

	Unit	$J = 6$			
$T_{W_1}$	(°C)	75.0	80.0	85.0	90.0
$T_{W_7}$	(°C)	58.1	51.1	41.7	41.4
$W_1$	(kg/s)	1940.8	1413.5	1087.0	905.2
$PR_{wh}$	(–)	2.3	2.9	3.4	3.8
Booster Position		2	4–5	2–6	3–6

The position of booster and the value of vapor generated by booster ( $V^w$ ) are strongly dependent upon heat source temperature ( $T_{W_1}$ ).

For low heat source temperature, the optimal positions of boosters tends be in the middle part of the system and the devices utilize most of remaining energy in the middle part as well. For high heat source temperature, the optimal positions of boosters become the latter part of the system. High heat source temperature gives the BMEE system ability

to operate at high top brine temperature and this can further exploit the remaining sensible heat, ergo the performance of the system is improved.



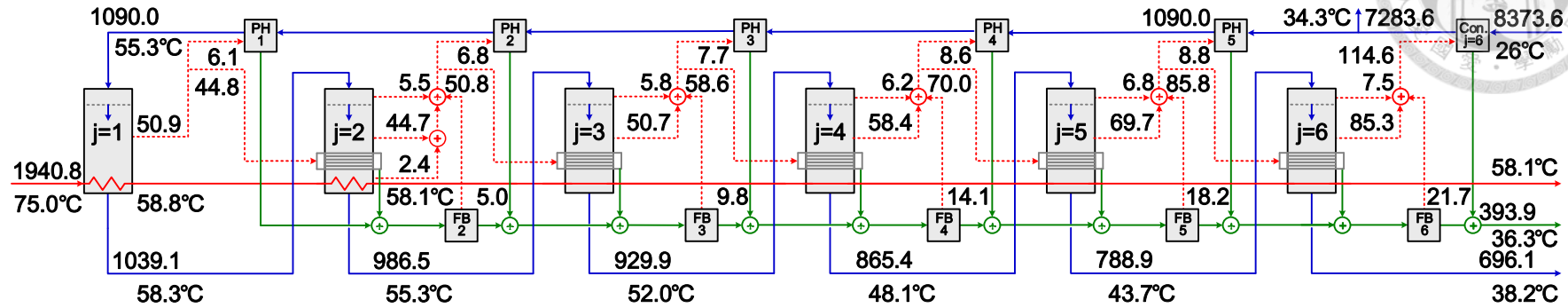
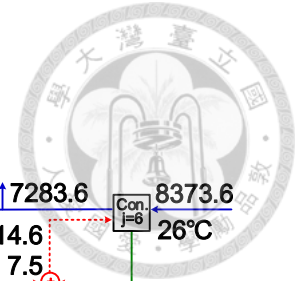


Figure 3.3: Optimal solution of BMEE system for Case 1 ( $T_{W_1} = 75^\circ\text{C}$ ).

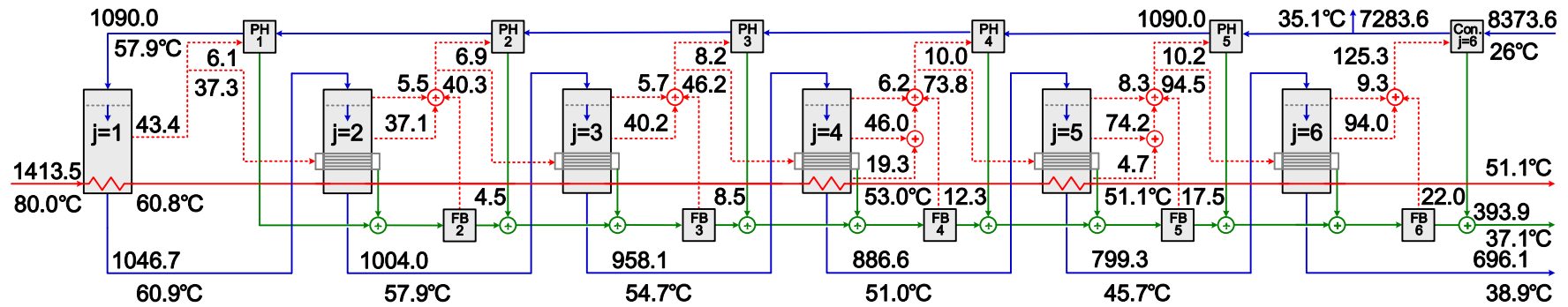


Figure 3.4: Optimal solution of BMEE system for Case 1 ( $T_{W_1} = 80^\circ\text{C}$ ).

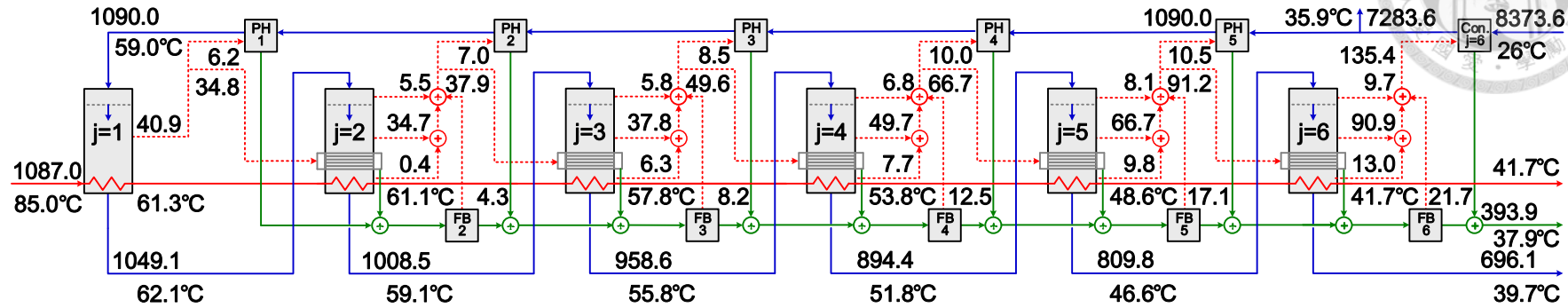
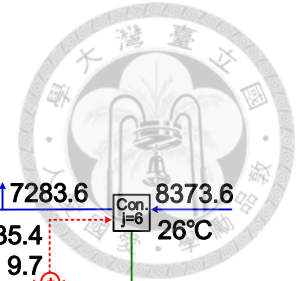


Figure 3.5: Optimal solution of BMEE system for Case 1 ( $T_{W_1} = 85^\circ\text{C}$ ).

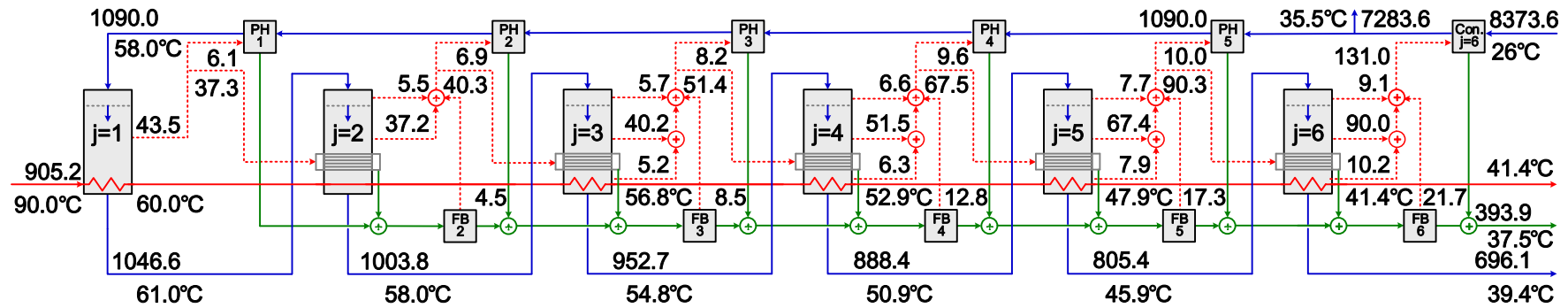


Figure 3.6: Optimal solution of BMEE system for Case 1 ( $T_{W_1} = 90^\circ\text{C}$ ).

### 3.3.2 Case 2: Influences of inlet temperature of heat source and number of effects

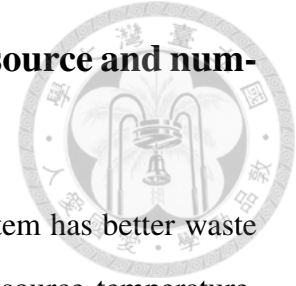


Figure 3.7 suggests that for same number of effects, BMEE system has better waste heat performance ratio compared with MEE system for high heat source temperature. However, for low heat source temperature, BMEE system has little improvement compared with MEE system due to energy requirement for producing demanded distillate.

The optimal number of effects should be decided by the heat source temperature. Despite the increase in the number of effects, for MEE (70 °C), the waste heat performance ratio performance decreased about 9%. Also for BMEE (75°C, 85°C and 90°C), the additional effect decreased the efficiency in exploitation of sensible heat.

Another advantage of BMEE system is shown in Figure 3.8. The required heat transfer area of BMEE system is prominently reduced by up to 14% comparing with MEE system. Details of heat transfer areas are provided in Table 3.3. The heat transfer area for first evaporator,  $A_1$ , is the summation of  $A_1^e$  and  $A_1^h$ . The reduction of  $A_1$  accounts for the reduction of  $A^{tot}$  in MEE system. However, the significantly decrease in the heat transfer area of evaporator is the major cause with regard to BMEE system.

Table 3.3: Detailed heat transfer areas.

	$J=6$							
	MEE				BMEE			
(1000m <sup>2</sup> )	75°C	80°C	85°C	90°C	75°C	80°C	85°C	90°C
$A_1$	7.5	6.7	6.2	5.8	7.4	6.2	5.7	5.2
$A_6^p$	18.1	18.1	18.1	18.1	18.2	19.0	19.7	19.4
$A^e$	98.6	98.6	98.6	98.6	94.4	77.5	72.1	77.6
$A^p$	7.0	7.0	7.0	7.0	7.1	7.1	7.1	7.1
$A^b$					0.6	3.7	7.5	6.0
$A^{tot}$	131.2	130.4	130.0	129.6	127.6	113.5	112.2	115.3

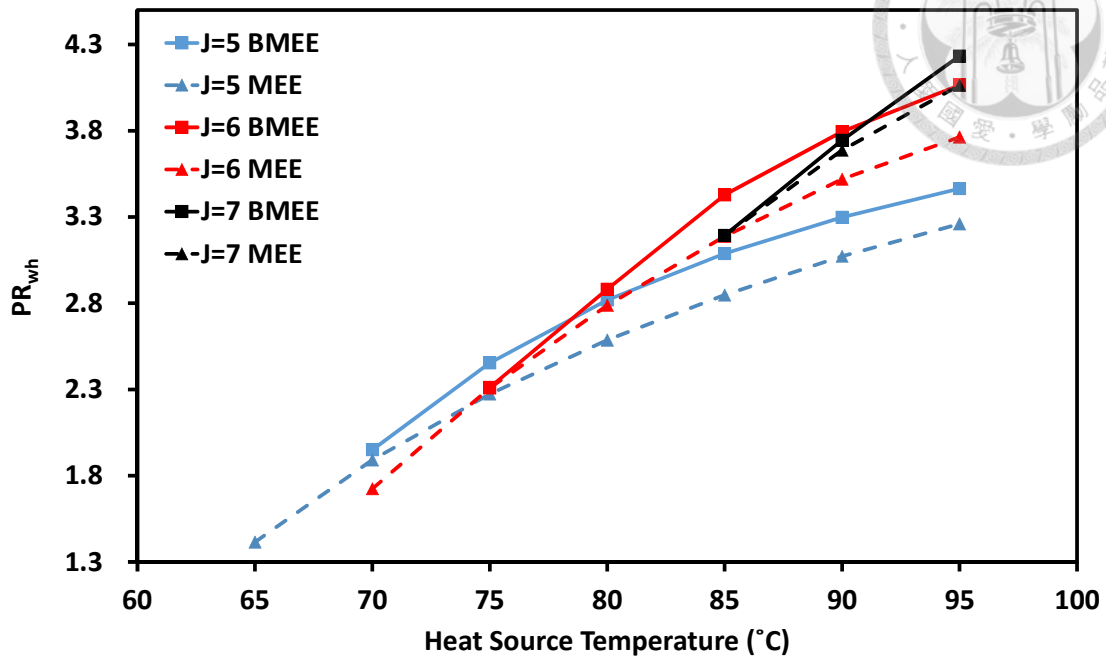


Figure 3.7: Waste heat performance ratio against heat source temperature.

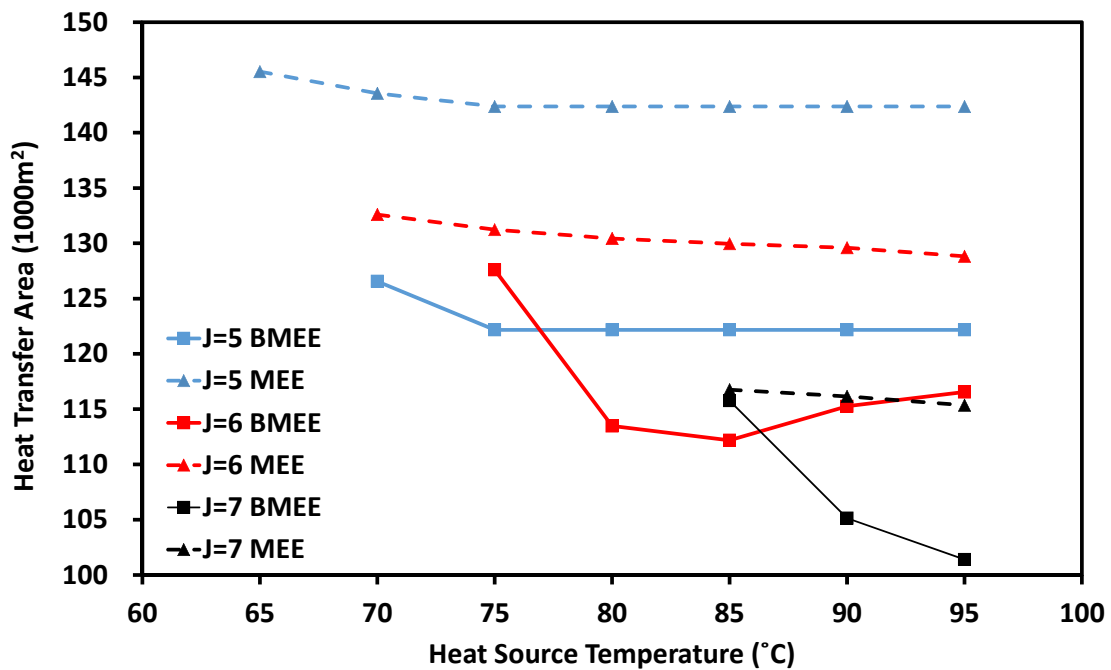
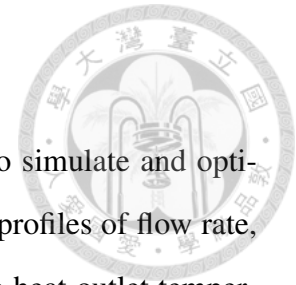


Figure 3.8: Heat transfer area against heat source temperature (the fresh water production is 393.94 kg/s).



### 3.4 Summary

A deterministic NLP mathematical model has been developed to simulate and optimize the BMEE system, which has ability to determine the optimal profiles of flow rate, heat transfer area, salinity and temperature. The influences of waste heat outlet temperature and number of effects on waste heat performance ratio were investigated. It was observed that the optimal waste heat outlet temperature were able to fall down to 41.4°C and waste heat performance ratio were enhanced. The BMEE system is superior to MEE system in both waste heat performance ratio and heat transfer area at higher inlet temperature of heat source.





## Chapter 4

# MEE/BMEE Systems for Waste Heat Recovery in Refinery

A practical demonstration on the design of MEE/BMEE systems is described in this chapter. Figure 4.1 is the case study about refinery [21, 22]. The sensible waste heat in a refinery is the heat source for MEE/BMEE systems. There are two goals that we pursue in this study. The primary goal is maximize the production of fresh water while satisfying specific waste heat sources. The secondary goal is to minimize the required cooling systems in Figure 4.1.

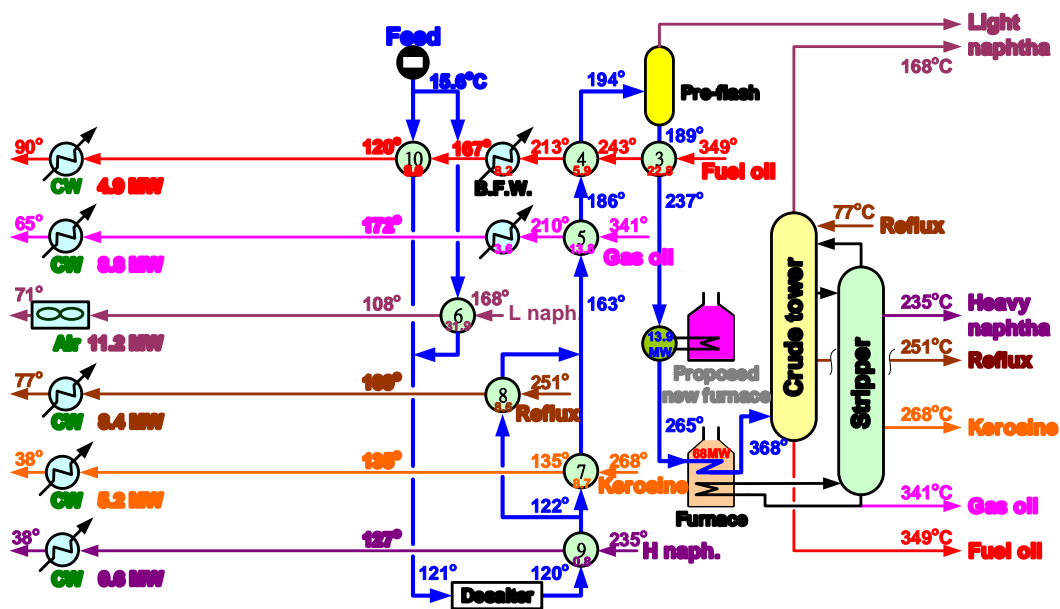
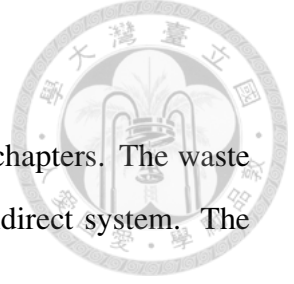


Figure 4.1: Typical crude preheat train with six waste hot streams.



## 4.1 Problem Statement

Both MEE system and BMEE system are described in previous chapters. The waste heat sources can be divided into two systems: direct system and indirect system. The heating medium in indirect system is assumed to be water.

Principally, waste heat sources are classified by the outlet temperature of waste heat. Given the fact that the first four streams have high outlet temperature, waste heat is recovered by indirect system where minimum temperature difference between heating medium and waste heat,  $\Delta T_{\min}^w$ , is  $10^\circ\text{C}$ .

To simplify the problem, the thermodynamic properties of heavy naphtha is identical to kerosine and the waste heat of heavy naphtha stream is collected by indirect system. Hence, kerosine stream is the only stream in direct system.

The upper limit for inlet temperature of indirect system is determined by light naphtha stream, that is  $T_{\text{ind}}^{\text{inlet}} = 98^\circ\text{C}$ ; the lower bound of inlet temperature of indirect system is determined by gas oil stream, that is  $T_{\text{ind}}^{\text{outlet}} = 55^\circ\text{C}$ .

## 4.2 Model Formulation

The model is based on MEE system, BMEE system and the waste sources in Figure 4.1.

### 4.2.1 Additional Models

The kerosine specific heat capacity [kJ/kg] at  $T_j$  [ $^\circ\text{C}$ ]:

$$C_p^{\text{kero}} = (1.8841 + 0.0038T_j) \quad (4.1)$$

Direct system:

$$D_{\text{dir}} = \left( \frac{D^{\text{tot}}}{W_1} \right)_{\text{dir}} \cdot W_{\text{dir}} \quad (4.2)$$

$$T_{\text{dir}}^{\text{inlet}} = (T_1)_{\text{dir}} \quad (4.3)$$

$$T_{\text{dir}}^{\text{outlet}} \leq (T_J)_{\text{dir}} \quad (4.4)$$



Eqs. (4.5) and Eqs. (4.6) are proposed to replace the original Eqs. (2.44) and Eqs. (2.45) for  $j \in \mathcal{J}, j = 1$

$$W_j(C_{p,W_j}^{\text{kero}} T_{W_j} - C_{p,W_j^s}^{\text{kero}} T_{W_j^s}) = V_j^w \lambda_j^w \quad (4.5)$$

$$W_j(C_{p,W_j^s}^{\text{kero}} T_{W_j^s} - C_{p,W_{j+1}}^{\text{kero}} T_{W_{j+1}}) = B_j (C_{p,B_{j+1}} T_{B_{j+1}} - C_{p,B_j} T_{B_j}) \quad (4.6)$$

Eqs. (4.7) is proposed to replace the original Eqs. (3.3) for  $j \in \mathcal{J}, j > 1$

$$V_j^w \lambda_j^w = W_j(C_{p,W_j}^{\text{kero}} T_{W_j} - C_{p,W_{j+1}}^{\text{kero}} T_{W_{j+1}}) \quad (4.7)$$

Indirect system:

$$W_{\text{ind}} = \left( \frac{Q}{C_{p,W_1} T_{W_1} - C_{p,W_J} T_{W_J}} \right)_{\text{ind}} \quad (4.8)$$

$$D_{\text{ind}} = \left( \frac{D^{\text{tot}}}{W_1} \right)_{\text{ind}} \cdot W_{\text{ind}} \quad (4.9)$$

$$T_{\text{ind}}^{\text{inlet}} = (T_1)_{\text{ind}} \quad (4.10)$$

$$T_{\text{ind}}^{\text{outlet}} \geq (T_J)_{\text{ind}} \quad (4.11)$$

## 4.2.2 NLP Formulation

Given a fixed number of effects, the proposed objective function for maximization is the freshwater production satisfying specific waste heat sources for different systems.

Table 4.1 lists the parameter values used for Chapter 4.



$$\max_{x \in \Omega} \Phi_{\text{dir}} = D_{\text{dir}}$$

$$\max_{x \in \Omega} \Phi_{\text{ind}} = D_{\text{ind}}$$

$$x \equiv \left\{ \begin{array}{l} A_j^b, A_j^e, A_1^h, A_j^p; \text{LMTD}_j^h, \text{LMTD}_j^p, \text{LMTD}_j^w; \\ V_j^e, V_j^f, V_j^g, V_j^p, V_j^w; \lambda_j, \lambda_j^e, \lambda_j^f, \lambda_j^g, \lambda_j^p, \lambda_j^w; \\ T_{V_j^e}, T_{V_j^f}, T_{V_j^g}, T_{V_j^p}, T_{V_j^w}; B_j, F_c, F_j, V_j, W_j; \\ T_{B_j}, T_{F_j}, T_{V_j}, T_{W_j}, T_{W_j^*}; X_{B_j}, X_{F_j}; \\ D_j, D_j^c, D_j^i, D_j^o, D_j^p; T_{D_j}, T_{D_j^c}, T_{D_j^i}, T_{D_j^o}, T_{D_j^p}; \\ D_{\text{dir}}, D_{\text{ind}}; W_{\text{dir}}, W_{\text{ind}}; \text{BPE}_j; C_p, C_p^{\text{kero}}; \\ H_{D_j}, H_{D_j^c}, H_{D_j^i}, H_{D_j^o}, H_{D_j^p}; \\ \forall j \in \mathcal{J} \equiv \{1, 2, \dots, J\} \end{array} \right.$$

$$\Omega = \{x \mid \text{Eqs. (2.1)-(2.63), Eqs. (3.1)-(3.7), Eqs. (4.1)-(4.11)}\}$$

Table 4.1: Parameter values.

Parameter	Unit	Value	Parameter	Unit	Value
$\Delta T_{\text{min}}$	(°C)	2.00	$U^a$	(kW)/(m <sup>2</sup> °C)	3.00
$\Delta T_{\text{min}}^e$	(°C)	3.00	$W_{\text{dir}}$	(kg/s)	21.09
$\Delta T_{\text{min}}^w$	(°C)	10.00	$T_{\text{dir}}^{\text{inlet}}$	(°C)	135
$D^{\text{tot } a}$	(kg/s)	393.94	$T_{\text{dir}}^{\text{outlet}}$	(°C)	38
$F_c^{\text{up } a}$	(kg/s)	7283.55	$Q_{\text{ind}}^{\text{up}}$	(MW)	33.75
$J$	(-)	6	$T_{\text{ind}}^{\text{inlet}}$	(°C)	98
$T^{\text{sea } a}$	(°C)	26.00	$T_{\text{ind}}^{\text{outlet}}$	(°C)	55
$X^{\text{sea } a}$	(ppm)	45,978.90	$T_{\text{ind}}^{\text{outlet } b}$	(°C)	56.77
$X^{\text{up } a}$	(ppm)	72,000.00			

<sup>a</sup> Numerical values from Druetta et al. [11]

<sup>b</sup> For indirect MEE system but with another bound due to the lowest possible waste heat outlet temperature constrained by cooling water and minimum temperature difference.

### 4.3 Case Study

Table 4.2 contains maximized freshwater production and corresponding heat transfer area for six different configurations. The configurations are shown in Figure 4.2 to Figure 4.7. The detailed profiles are shown in Figure 4.8 to Figure 4.13. The optimal configuration is that of direct BMEE system along with indirect MEE system considering maximum production of fresh water.

From the aspects of thermodynamics, MEE system utilize the waste heat only in first effect which is superior to BMEE system in conventional performance ratio. As the specified waste heat outlet temperature is higher than the lowest possible waste heat outlet temperature of MEE system, it become more appropriate to use MEE system rather than BMEE system.

Nevertheless, the available waste heat as described in Section 1.4, increases as the specified waste heat outlet temperature decreases. MEE system fails to make use of the additional energy due to the limit of lowest possible temperature discussed in Chapter 2. In Chapter 3, BMEE system has shown the capability to fully utilize the sensible waste heat at low specified waste heat outlet temperature.

The ideal configuration of Figure 4.1 would be six direct system. However, it is quite infeasible for typical factories since there is no sufficient space available. Indirect system, which is more space-saving, can collect waste heat from diverse sources and generate fresh water with slightly decreased efficiency.

In conclusion, the outlet temperature of waste heat is the key to choose either MEE system or BMEE system in terms of freshwater production. As the outlet temperature of waste heat is lower than the lowest possible waste heat outlet temperature of MEE system, BMEE system is more favorable than the other.



Table 4.2: Comparison for different configurations.

Parameter	Direct		MEE		BMEE		
	Indirect	MEE	BMEE	MEE	BMEE	MEE	BMEE
$A_{dir}$	(1000m <sup>2</sup> )			4.0	4.0	4.0	4.0
$A_{ind}$	(1000m <sup>2</sup> )	34.9	33.4	31.4	30.0	31.4	30.0
$A^{tot}$	(1000m <sup>2</sup> )	34.9	32.4	35.4	34.0	35.4	34.0
$D_{dir}$	(kg/s)			12.3	12.3	13.0	13.0
$D_{ind}$	(kg/s)	107.1	105.5	96.2	94.6	96.2	94.6
$D^{tot}$	(kg/s)	107.1	105.5	108.5	106.9	109.2	107.6
$W_{ind}$	(kg/s)	213.1	205.9	191.4	184.6	191.4	184.6

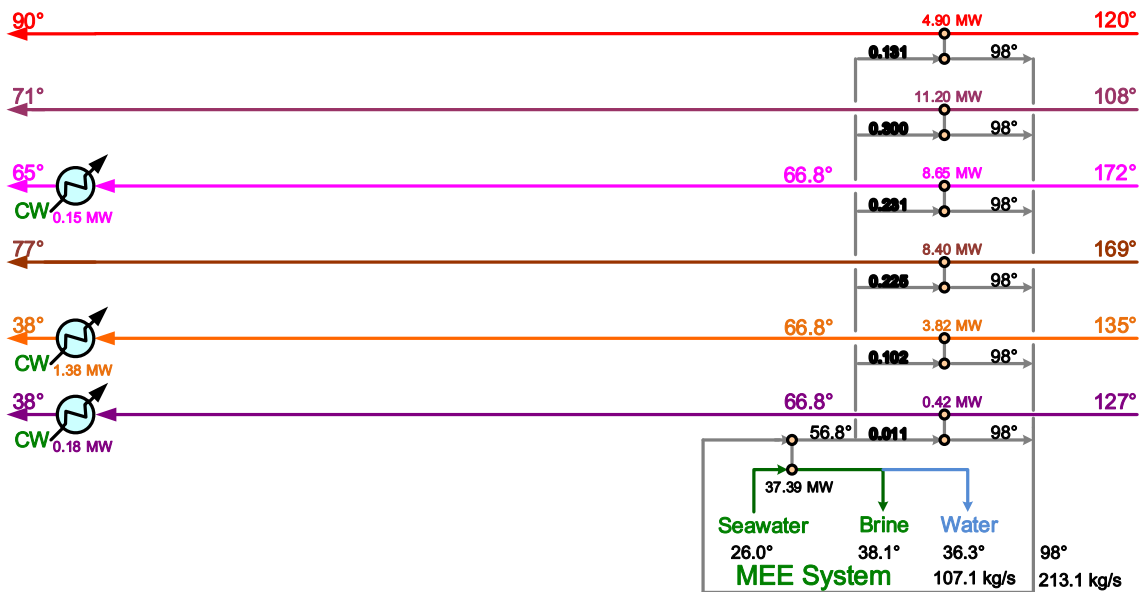


Figure 4.2: Indirect MEE system.

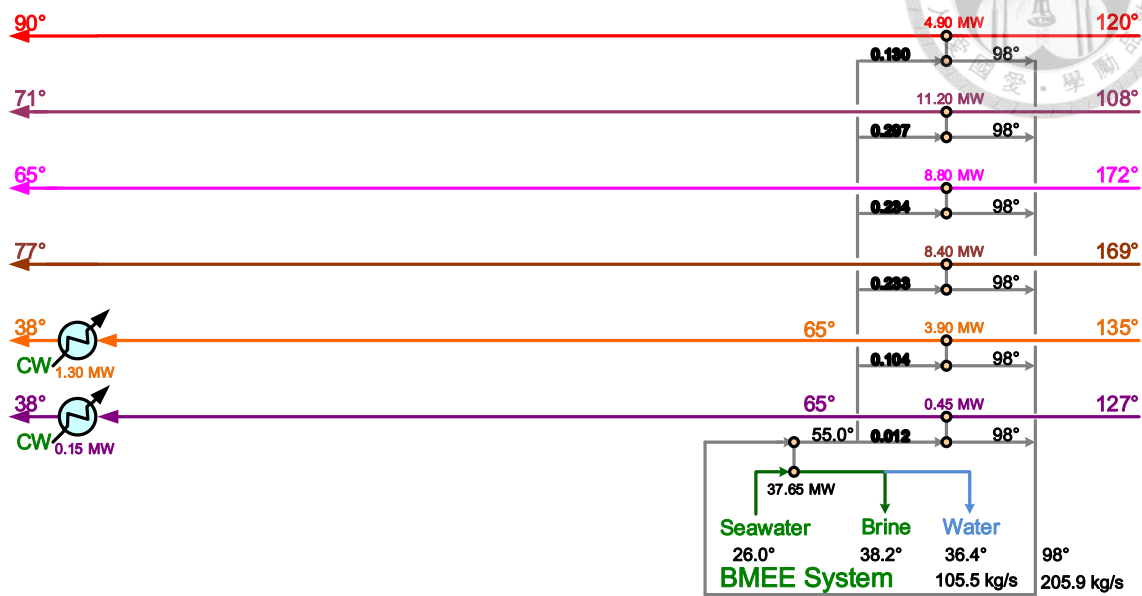
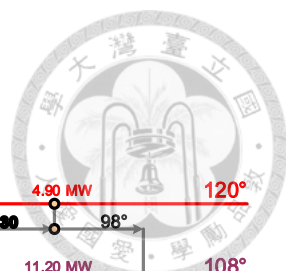


Figure 4.3: Indirect BMEE system.

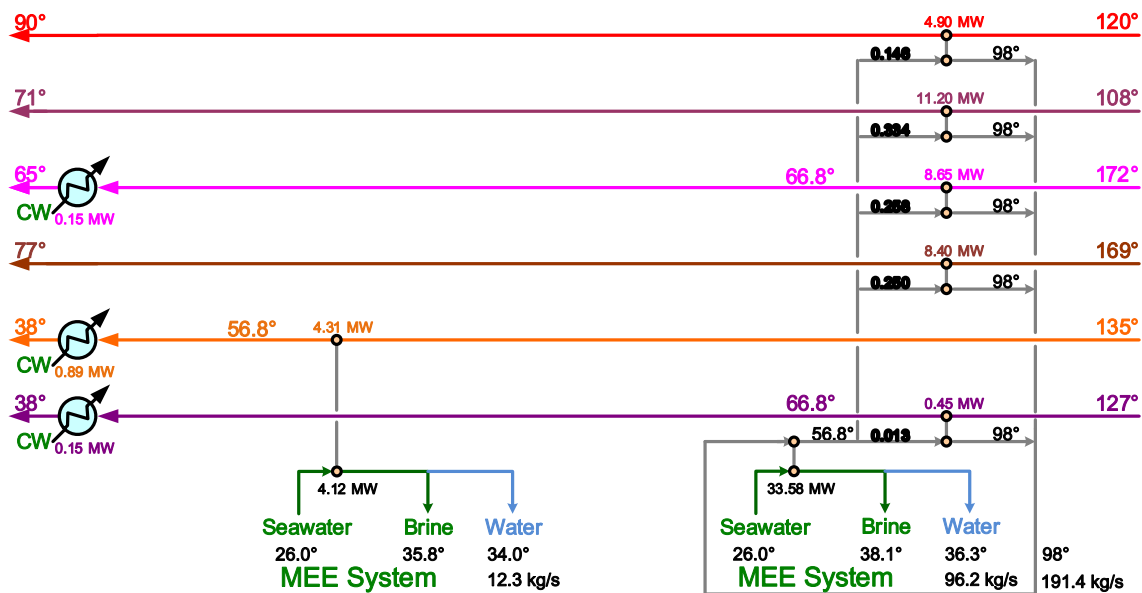


Figure 4.4: Direct MEE system and indirect MEE system.



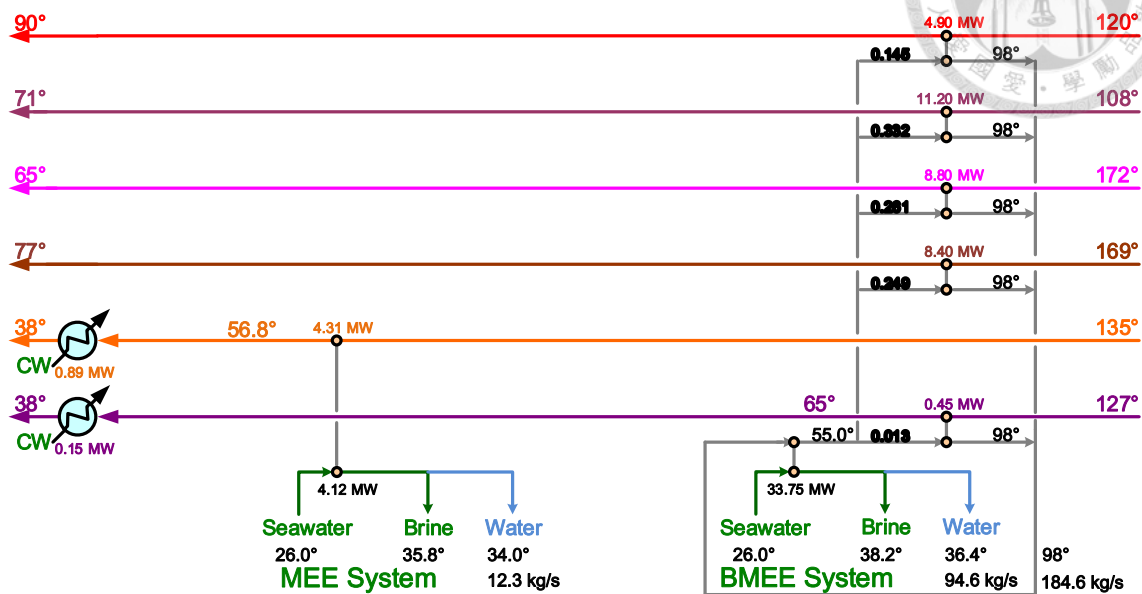
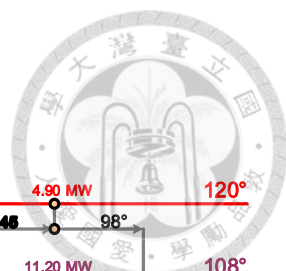


Figure 4.5: Direct MEE system and indirect BMEE system.

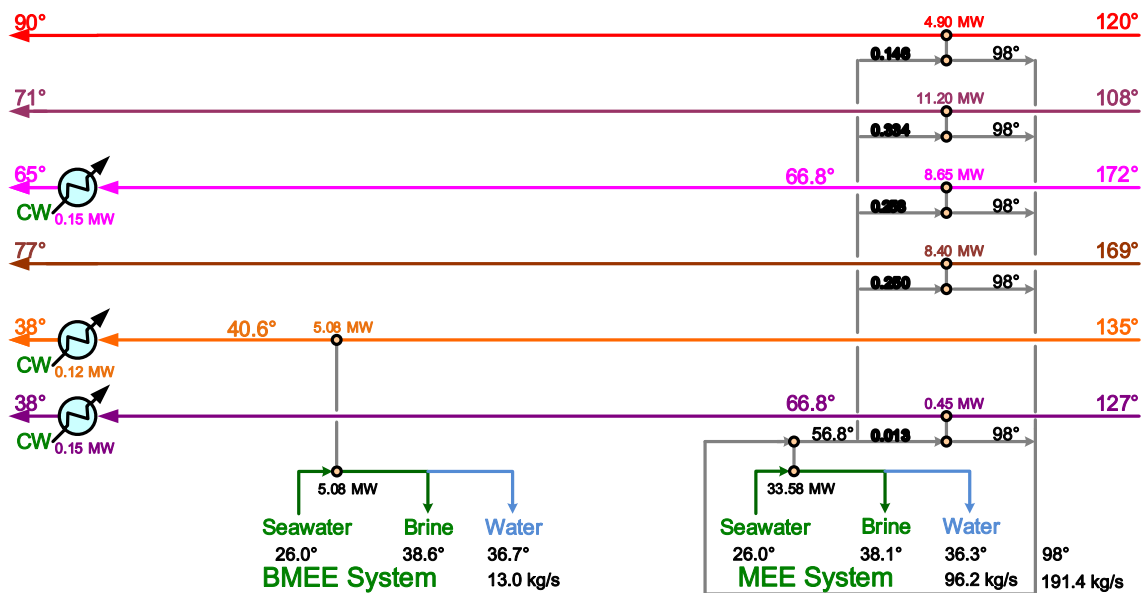


Figure 4.6: Direct BMEE system and indirect MEE system.

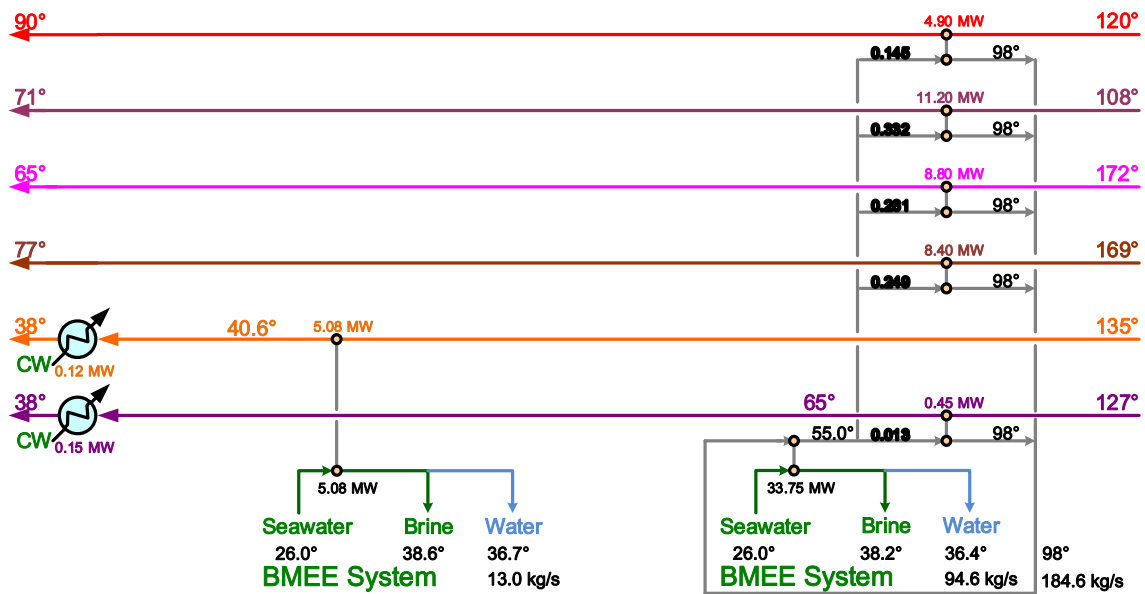


Figure 4.7: Direct BMEE system and indirect BMEE system.

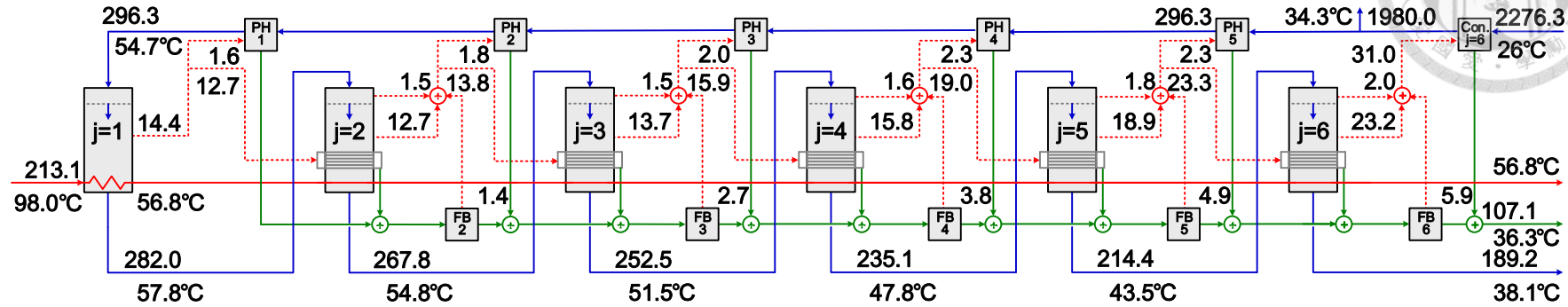
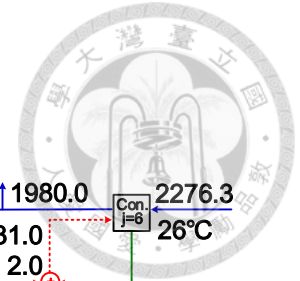


Figure 4.8: Details of indirect MEE system in Figure 4.2.

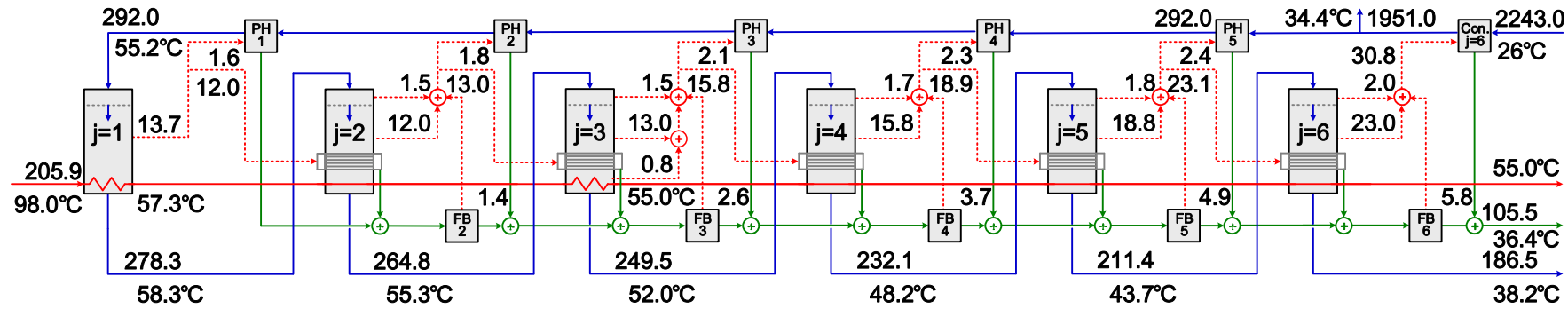


Figure 4.9: Details of indirect BMEE system in Figure 4.3.

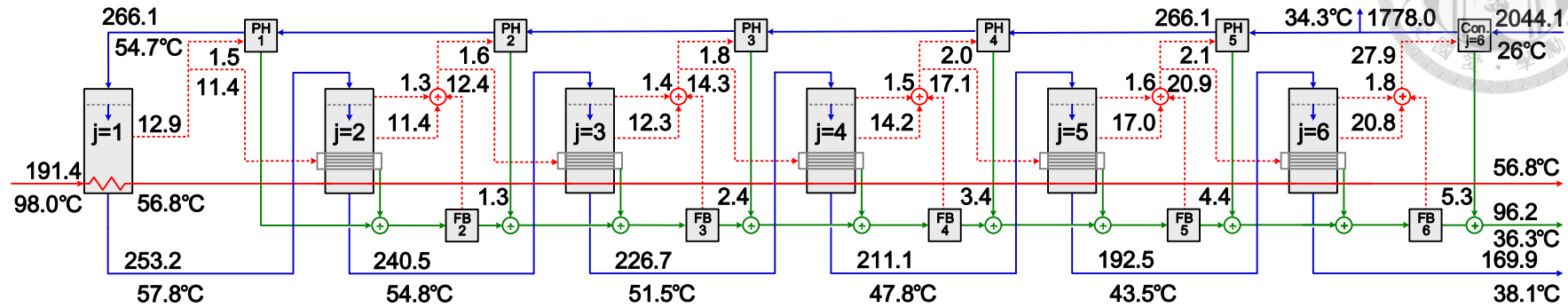
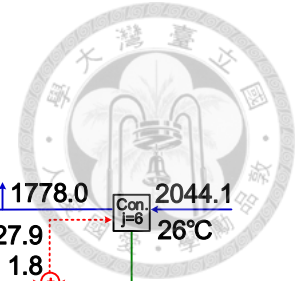


Figure 4.10: Details of indirect MEE system in Figure 4.4 and Figure 4.6.

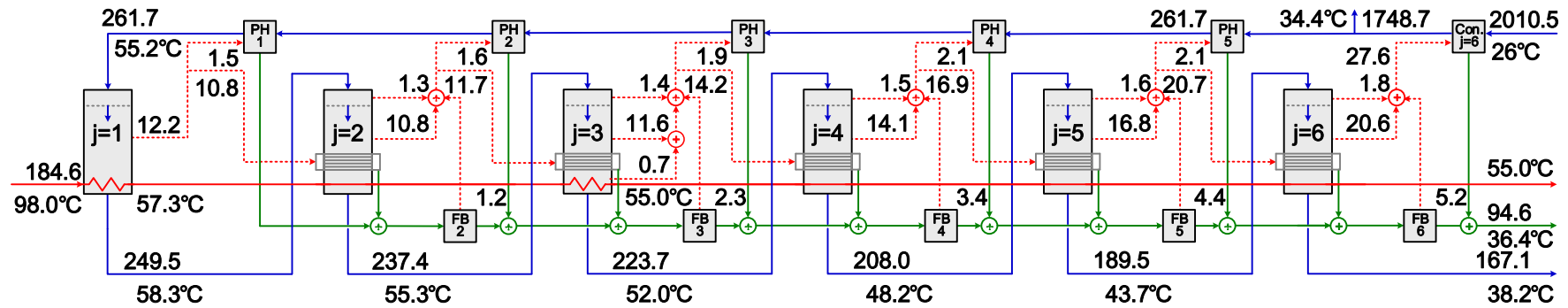


Figure 4.11: Details of indirect BMEE system in Figure 4.5 and Figure 4.7.

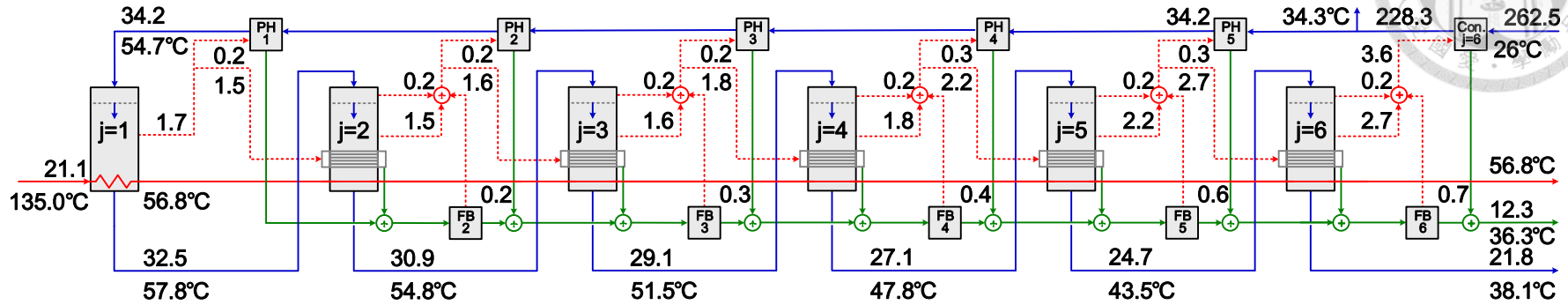
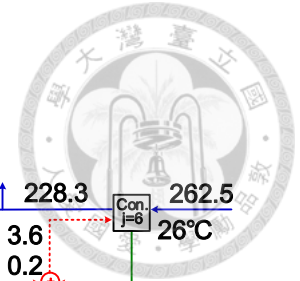


Figure 4.12: Details of direct MEE system in Figure 4.4 and Figure 4.5.

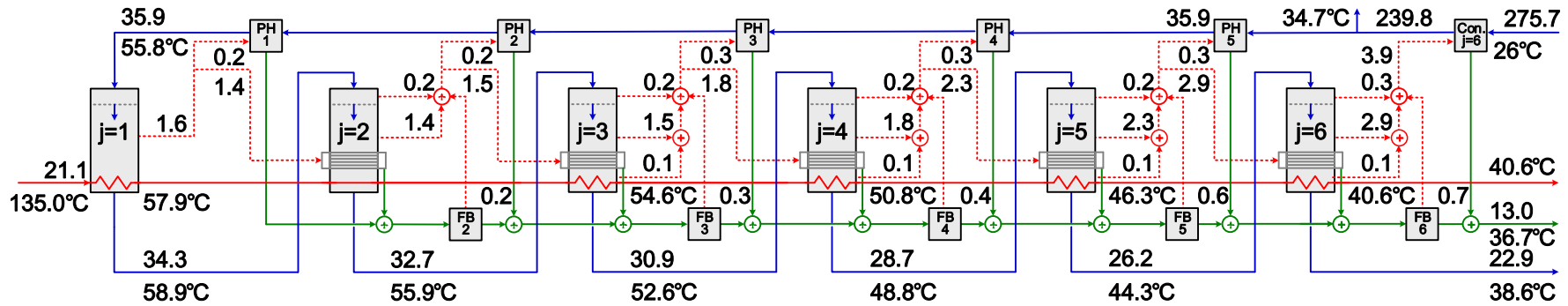


Figure 4.13: Details of direct BMEE system in Figure 4.6 and Figure 4.7.



## Chapter 5

### Conclusion

In this work, deterministic NLP mathematical models have been developed to simulate and optimize MEE system and BMEE system, which has ability to determine the optimal profiles of flow rate, heat transfer area, salinity and temperature.

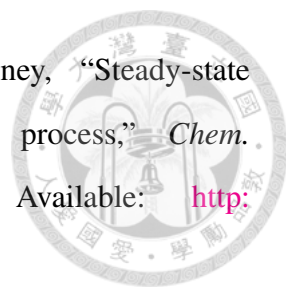
The influences of waste heat outlet temperature and number of effects on waste heat performance ratio were investigated for both systems. It was concluded that the leaving temperature was quite high and the waste heat could not be efficiently exploited by MEE system. Therefore, BMEE system was studied and the results showed that BMEE system is superior to MEE system in both waste heat performance ratio (up to 8%) and heat transfer area (up to 14%). BMEE system has shown the capability to fully utilize the sensible waste heat at low specified waste heat outlet temperature.

The outlet temperature of waste heat is the key to choose either MEE system or BMEE system in terms of freshwater production. While the specified waste heat outlet temperature is higher than the lowest possible temperature of MEE system, it become more appropriate to use MEE system rather than BMEE system.

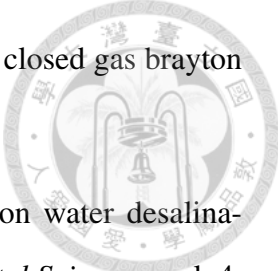


## Bibliography

- [1] U.N. Water, "Water and energy," *World water development report 2014*, vol. 1, pp. 2–7, 2014. [Online]. Available: <http://www.unesco.org/new/en/natural-sciences/environment/water/wwap/wwdr/2014-water-and-energy/>
- [2] B. W. Eakins and G. F. Sharman, "Volumes of the world's oceans from etopo1," *NOAA National Geophysical Data Center*, 2010.
- [3] THE WORLD BANK, "Renewable internal freshwater resources per capita," *Food and Agriculture Organization, AQUASTAT data*, 2014. [Online]. Available: <https://data.worldbank.org/indicator/ER.H2O.INTR.PC>
- [4] World Economic Forum, "Global risks report 2017," p. 18, 2017. [Online]. Available: [http://www3.weforum.org/docs/GRR17\\_Report\\_web.pdf](http://www3.weforum.org/docs/GRR17_Report_web.pdf)
- [5] M. M. Mekonnen and A. Y. Hoekstra, "Four billion people facing severe water scarcity," *Science Advances*, vol. 2, no. 2, 2016. [Online]. Available: <http://advances.sciencemag.org/content/2/2/e1500323>
- [6] IEA-ETSAP and IRENA, "Water desalination using renewable energy: Technology brief," 2012. [Online]. Available: [www.irena.org/Publications](http://www.irena.org/Publications)
- [7] DesalData, "Worldwide desalination inventory (ms excel format)," 2014.
- [8] DESWARE, "Energy requirements of desalination processes," 2013. [Online]. Available: <http://www.desware.net/Energy-Requirements-Desalination-Processes.aspx>

- 
- [9] H. El-Dessouky, I. Alatiqi, S. Bingulac, and H. Ettouney, “Steady-state analysis of the multiple effect evaporation desalination process,” *Chem. Eng. Technol.*, vol. 21, pp. 437–451, 1998. [Online]. Available: [http://refhub.elsevier.com/S0011-9164\(16\)30435-0/rt0130](http://refhub.elsevier.com/S0011-9164(16)30435-0/rt0130)
- [10] K. H. Mistry, M. A. Antar, and J. H. Lienhard, “An improved model for multiple effect distillation,” *Desalination and Water Treatment*, vol. 51, no. 4-6, pp. 807–821, 2013. [Online]. Available: [GotoISI://WOS:000313794400017](http://GotoISI://WOS:000313794400017)
- [11] P. Druetta, P. Aguirre, and S. Mussati, “Optimization of multi-effect evaporation desalination plants,” *Desalination*, vol. 311, pp. 1–15, 2013. [Online]. Available: [GotoISI://WOS:000315012500001](http://GotoISI://WOS:000315012500001)
- [12] A. Christ, K. Regenauer-Lieb, and H. T. Chua, “Boosted multi-effect distillation for sensible low-grade heat sources: A comparison with feed pre-heating multi-effect distillation,” *Desalination*, vol. 366, pp. 32–46, 2015. [Online]. Available: [GotoISI://WOS:000355035100005](http://GotoISI://WOS:000355035100005)
- [13] A. Christ, X. Wang, K. Regenauer-Lieb, and H. T. Chua, “Low-grade waste heat driven desalination technology,” *International Journal for Simulation and Multidisciplinary Design Optimization*, vol. 5, 2014. [Online]. Available: [http://refhub.elsevier.com/S0011-9164\(16\)30435-0/rt0110](http://refhub.elsevier.com/S0011-9164(16)30435-0/rt0110)
- [14] B. Rahimi, A. Christ, K. Regenauer-Lieb, and H. T. Chua, “A novel process for low grade heat driven desalination,” *Desalination*, vol. 351, pp. 202–212, 2014. [Online]. Available: [GotoISI://WOS:000342248800022](http://GotoISI://WOS:000342248800022)
- [15] X. L. Wang, A. Christ, K. Regenauer-Lieb, K. Hooman, and H. T. Chua, “Low grade heat driven multi-effect distillation technology,” *International Journal of Heat and Mass Transfer*, vol. 54, no. 25-26, pp. 5497–5503, 2011. [Online]. Available: [GotoISI://WOS:000296035300036](http://GotoISI://WOS:000296035300036)



- 
- [16] H. Zhao and P. Peterson, “Advanced med using waste heat from closed gas brayton cycles,” *Transactions of the ANS*, vol. 96, pp. 791–792, 2007.
- [17] S. M. Alcocer and G. Hiriart, “An applied research program on water desalination with renewable energies,” *American Journal of Environmental Sciences*, vol. 4, no. 3, pp. 204–211, 2008.
- [18] A. Christ, K. Regenauer-Lieb, and H. T. Chua, “Application of the boosted med process for low-grade heat sources — a pilot plant,” *Desalination*, vol. 366, pp. 47 – 58, 2015. [Online]. Available: <http://www.sciencedirect.com/science/article/pii/S0011916414005554>
- [19] H. R. Dastgerdi, P. B. Whittaker, and H. T. Chua, “New med based desalination process for low grade waste heat,” *Desalination*, vol. 395, pp. 57–71, 2016. [Online]. Available: [GotoISI://WOS:000379637400008](http://www.sciencedirect.com/science/article/pii/S0011916414005554)
- [20] A. Christ, K. Regenauer-Lieb, and H. T. Chua, “Thermodynamic optimisation of multi effect distillation driven by sensible heat sources,” *Desalination*, vol. 336, pp. 160 – 167, 2014. [Online]. Available: <http://www.sciencedirect.com/science/article/pii/S0011916413005791>
- [21] C. L. Chen, P. Y. Li, and S. N. T. Le, “Organic rankine cycle for waste heat recovery in a refinery,” *Industrial & Engineering Chemistry Research*, vol. 55, no. 12, pp. 3262–3275, 2016. [Online]. Available: <https://doi.org/10.1021/acs.iecr.5b03381>
- [22] I. C. Kemp, *Pinch analysis and process integration*, 2nd ed. Elsevier, 2007.